

1 **A standardized index for assessing sub-monthly compound**
2 **dry and hot conditions: with application in China**

3 Jun Li¹, Zhaoli Wang^{1,2}, Xushu Wu^{1,2,*}, Jakob Zscheischler^{3,4,5}, Shenglian Guo⁶,
4 Xiaohong Chen⁷

5 ¹ *School of Civil Engineering and Transportation, State Key Laboratory of Subtropical*
6 *Building Science, South China University of Technology, Guangzhou 510641, China.*

7 ² *Guangdong Engineering Technology Research Center of Safety and Greenization for*
8 *Water Conservancy Project, Guangzhou 510641, China.*

9 ³ *Climate and Environmental Physics, University of Bern, Sidlerstrasse 5, 3012 Bern,*
10 *Switzerland.*

11 ⁴ *Oeschger Centre for Climate Change Research, University of Bern, Bern, Switzerland.*

12 ⁵ *Department of Computational Hydrosystems, Helmholtz Centre for Environmental*
13 *Research - UFZ, Leipzig, Germany.*

14 ⁶ *State Key Laboratory of Water Resources and Hydropower Engineering Science,*
15 *Wuhan University, Wuhan 430072, China.*

16 ⁷ *Center for Water Resource and Environment, Sun Yat-Sen University, Guangzhou*
17 *510275, China.*

18 **Correspondence: xshwu@scut.edu.cn.*

19

20

21

22

23

24 **Abstract:** Compound dry and -hot conditions ~~pose~~ frequently cause large impacts on
25 ecosystems and societies worldwide. A suite of indices ~~are~~ are available ~~proposed~~
26 the assessments of droughts and heatwaves ~~previously~~, yet there is no index available
27 for incorporating the joint variability of dry and hot conditions at sub-monthly scale.
28 Here, we introduced a daily-scale index, ~~termed~~ as called the standardized compound
29 drought and heat index (SCDHI), to ~~measure~~ assess ~~the intensity of~~ compound dry ~~and~~
30 ~~hot~~ conditions. The SCDHI is based on ~~the~~ a daily drought index (the standardized
31 antecedent precipitation evapotranspiration index (SAPEI)) ~~and~~, the daily-scale
32 standardized temperature index (STI) and a joint probability distribution method. The
33 new index ~~is~~ was verified against real-world compound dry and hot events and ~~the~~
34 ~~associated~~ related observed vegetation impacts in China. The SCDHI can not only
35 capture compound dry and hot events at both monthly and sub-monthly scales, but is
36 also a good indicator for associated vegetation impacts. ~~SCDHI can not only monitor~~
37 ~~the long term compound dry and hot events, but also capture such events at sub-~~
38 ~~monthly scale and reflect the related vegetation activity impacts.~~ Using the SCDHI, we
39 quantify the mean frequency, severity, duration and intensity of compound dry-hot
40 events during the historical period in China and assess the ability of climate models to
41 reproduce these characteristics. We find that the compound events whose severity is at
42 least light and which last longer than two weeks generally persisted for ~~25~~ 20-35 days
43 in China. ~~;~~ ~~and the~~ southern China ~~suffers~~ suffered from compound events most
44 frequently, and the most severe compound events were mainly detected in this region.
45 Climate models generally overestimate the frequency, duration, severity and intensity
46 of compound events in China, especially for western regions, which can be attributed
47 to a too strong dependence between the SAPEI and STI in those models. ~~SCDHI index~~
48 ~~can~~ The SCDHI provides a new tool to quantify sub-monthly characteristics of

49 compound dry and hot events, ~~and conducive to the timely monitoring of~~ their initiation,
50 development, and decay. ~~which This is important information are vital~~ for decision-
51 makers and stake-holders to release early and timely warnings.

52 **Keywords:** compound event; SCDHI; SAPEI; sub-monthly scale; China

53 1 Introduction

54 Compound dry-hot events are climate events during which dry and hot conditions
55 occur simultaneously. ~~Compound dry-hot event, and such events~~ have been observed
56 ~~for on~~ all continents in recent decades (Hao et al., 2019; Mazdidasni and AghaKouchak,
57 2015; Manning et al., 2019; Sutanto et al., 2020). ~~The frequent e~~Compound dry-hot
58 events ~~have can~~ lead to more devastating impacts on natural ecosystems and human
59 society ~~than compared to droughts and heatwaves alone individual events~~ (Zscheischler
60 et al., 2014, ~~2018~~; Chen et al., 2019; Hao et al., 2018a). For example, Russia was
61 simultaneously struck by a severe drought and unrepresented temperature extremes in the
62 summer of 2010, which caused large-scale crop failures, wildfires, and human mortality
63 (Zscheischler et al., 2018). ~~Unfortunately, the extreme droughts and hots~~ Droughts and
64 heatwaves are expected to occur more frequently in the coming decades under global
65 warming, which potentially results in more compound events in many parts of the world,
66 especially for wet and humid regions (Wu et al., 2020; Swain et al., 2018, Zscheischler
67 and Seneviratne, 2017a). Therefore, understanding such events ~~are is~~ of crucial
68 importance to provide ~~the most fundamental~~ relevant information ~~to help for~~
69 mitigation.

70 ~~Much effort has been made to study the~~ Many studies have investigated multivariate
71 compound events in recent years (Zscheischler et al., 2020; Ridder et a., 2020).
72 Utilizing ~~different~~ thresholds to define ~~the~~ concurrent climate extremes for a specific

73 period, particularly the frequency of multivariate compound events has received ~~a great~~
74 ~~deal of~~ a lot of attention (Wu et al., 2019; Zhang et al., 2019; Ridder et al., 2020).
75 However, for impacts, ~~Although this approach can detect compound event occurrence,~~
76 ~~it the method of frequency analysis other fails to quantitatively measure~~ compound
77 event characteristics such as duration, severity, and intensity may be at least as
78 important, and may help ~~is inconvenient for comparison of~~ to compare compound event
79 characteristics ~~through~~ across different climates (Wu et al., 2020). ~~Therefore,~~ To
80 overcome these ~~shortages~~ limitations, several joint climate extreme indices have been
81 proposed for analyzing ~~the~~ characteristics of ~~the~~ compound events beyond frequency.
82 ~~Specifically~~ For instance, the standardized dry and hot index based on the ratio of the
83 marginal probability distribution functions of precipitation and temperature was
84 proposed to measure the extreme ness ~~degree~~ of a compound drought and hot ~~extreme~~
85 event (Hao et al., 2018). Hao et al. (2019, 2020) recently proposed the standardized
86 compound event indicator and compound dry-hot index to assess the severity of
87 compound dry and hot events by ~~jointing~~ linking the marginal distribution of
88 standardized precipitation index (SPI) and standardized temperature index (STI) using
89 ~~the~~ copula theory. These two joint indices provide useful tools to improve our
90 understanding of the frequency, spatial extent and severity of ~~the~~ compound dry-hot
91 events s. ~~However, they are inevitably subjected to some shortcomings including the~~
92 ~~fixed monthly scale and the disregard of evapotranspiration, which may limit their use~~
93 ~~in monitoring the detailed evolution of compound dry and hot events.~~

94 ~~With the occurrence of extreme climate (e.g. high temperature, low humidity, and~~
95 ~~sunny skies), droughts can evolve rapidly~~ (Koster et al., 2019; Otkin et al., 2018; Yuan
96 et al., 2019; Li et al., 2020a). Such extreme weather can appear within a short period
97 ~~without resulting in long-lasting compound events, but rather, short term droughts and~~

98 ~~heatwaves lasting a few weeks or even days (Mo and Lettenmaier, 2016; Zhang et al.,~~
99 ~~2019). Severe concurrent drought and heat can suddenly strike a region with a relatively~~
100 ~~short duration when extreme weather anomalies persist over the same region~~
101 ~~(Röthlisberger and Martius, 2019; Wang et al., 2016). Concurrent~~ However, when
102 extreme weather conditions (e.g., high temperature, low humidity, and sunny skies)
103 occur within a short period, droughts can evolve rapidly, in conjunction with heatwaves
104 (Koster et al., 2019; Otkin et al., 2018; Pendergrass et al. 2020; Yuan et al., 2019; Li et
105 al., 2020a). Despite their short duration, concurrent short-term drought and hot
106 extremes can pose ~~greater potential~~ large socio-economic risks because the combination
107 of ~~these both hazards events~~ can exacerbate their respective environmental and societal
108 impacts (Kirono et al., 2017; Schumacher et al., 2019; Sedlmeier et al., 2018).
109 ~~Specifically,~~ For instance, even short-term concurrent dry and hot extremes can lead to
110 significant agricultural loss if they occur within sensitive stages in crop development
111 such as emergence, pollination, and grain filling (Haqiqi et al., 2021; Luan and Vico et
112 al., 2021; Zhang et al., 2019). Under climate change, short-term concurrent dry and hot
113 extremes are expected to increase (especially for humid regions), potentially causing
114 substantial damage to natural ecosystems and society (Li et al., 2020b; Sun et al., 2019).
115 To improve understanding of such short-term compound events and ~~make issue~~ early
116 and timely warnings, decision-makers and stakeholders require more detailed
117 information such as the start time, severity, and the projected ~~projected~~ tendency in for
118 the coming days rather than the average state at a fixed monthly scale (Pendergrass et
119 al., 2020). However, the above-mentioned indices often only allow for identifying
120 compound dry-hot events at a relatively coarse (i.e., the monthly) temporal resolution
121 (Hao et al., 2019, 2020). and key characteristics of climate extremes may not be
122 detectable at monthly scale (Lu, 2019; Lu et al., 2014; Otkin et al., 2018). For instance,

123 [hot extremes generally occur at much finer time scales \(e.g., days and weeks\) \(Zhang](#)
124 [et al., 2019\).](#) ~~Correspondingly~~ [Consequently](#), sub-monthly-scale indices for
125 characterizing short-term compound dry and hot ~~events-conditions~~ are needed. In
126 addition, through the influence of evapotranspiration, ~~short-term~~ [other](#) meteorological
127 variables [that vary at short time scales](#) (e.g., [relative humidity, wind speed, and](#)
128 [radiation](#) ~~temperature and radiation~~) ~~are considered an important factor in~~ [may be](#)
129 [important drivers of](#) drought and heatwave concurrences (James et al., 2010). Thus, the
130 development of a compound drought and heat index should consider other important
131 ~~drought/hot related factors including temperature and~~ [variables such as](#)
132 evapotranspiration.

133 ~~The complexity of compound events makes it an unusual task to develop a simple~~
134 ~~and robust index to quantify their past and future changes (Zscheischler et al., 2020). A~~
135 ~~suite of indices are proposed for the assessments of droughts and heatwaves previously,~~
136 ~~yet there is no index available for incorporating the joint variability of dry and hot~~
137 ~~conditions at sub-monthly scale.~~ Here we ~~aim to formulate~~ [develop](#) a compound drought
138 and heat index, called the standardized compound drought and heat index (SCDHI), for
139 monitoring ~~and analyzing~~ compound dry and hot events at sub-monthly scale. To
140 achieve this aim, we combine a daily scale drought index, the standardized antecedent
141 precipitation evapotranspiration index (SAPEI), which simultaneously considers
142 precipitation and potential evapotranspiration, with a daily-scale standardized
143 temperature index (STI). [The SCDHI provides a new tool to quantify various](#)
144 [characteristics of compound dry-hot events, and can be computed at multiple time scale](#)
145 [\(e.g., daily, weekly and monthly\).](#)

146 [Several studies have been carried out to study compound dry-hot event in China](#)
147 [\(Chen et al., 2019; Hao et al., 2019; Wu et al., 2020; Zhang et al., 2019; Zhou and Liu,](#)

148 2018), and these studies help to better understand such events. However, they mostly
149 focused on the frequency and severity of the compound dry-hot event at a relatively
150 coarse (i.e., the monthly) temporal resolution without considering their duration and
151 intensity. ~~In addition, the impact of climate change on compound dry-hot event and its~~
152 ~~future change in China remains unclear.~~In addition, the effect of climate model bias on
153 the characteristics of compound dry-hot event in China remains unclear. Understanding
154 climate model biases is a crucial step to assess the risk of future compound dry-hot
155 events (Villalobos-Herrera et al., 2020). Recent compound dry-hot events have resulted
156 in serious social and economic losses in China (Wu et al., 2020; Zhang et al., 2019),
157 motivating further study of these potentially very damaging events. Using the SCDHI,
158 here we investigate ~~important~~the characteristics such as frequency, duration, severity,
159 and intensity of compound dry-hot events during the historical (1961-2018) period and
160 evaluate the effect of climate model biases on compound event characteristics in
161 China. ~~project their changes in China for the future (2050-2100) under different~~
162 ~~emission scenarios. This index can provide a new tool to quantify the characteristics of~~
163 ~~compound dry-hot event, and can monitor the compound dry-hot event at multiple time~~
164 ~~scale (e.g., daily, weekly and monthly) to provide detailed information on their~~
165 ~~initiation, development, decay, and trends.~~

166 The paper is organized as follows: Section 2 introduces the data used in this study,
167 the development of SCDHI. In the Section 3, the validation of SAPEI and SCDHI are
168 presented and characteristics of compound dry-hot event and the impact of climate
169 model bias on its characteristic are investigated. The study is concluded in Section 4.

170 2. Data and methodology**Methods**

171 **2.1 ~~data~~Data**

172 Daily meteorological datasets covering 1961 to 2018 were collected from 2239

173 observational stations across the non-arid region in China (Fig. 1), which include
174 precipitation, maximum air temperature, mean air temperature, minimum air
175 temperature, relatively humidity, wind speed, and sunshine duration. ~~All of these~~
176 ~~meteorological~~The data with strict quality control are available from the China
177 Meteorological Administration (<http://cdc.nmic.cn/home.do>) and the Resources and
178 Environmental Science Data Center, Chinese Academy of Sciences
179 (<http://www.resdc.cn/Default.aspx>). The observational station data were interpolated to
180 $0.25 \times 0.25^\circ$ gridded data by kriging ~~method~~, as it yields higher interpolation accuracy
181 than the other commonly used methods, e.g., ordinary nearest neighbor and inverse
182 distance weighting (Liu et al., 2016). In this study, we only focus the non-arid region
183 in China, because of three reasons: (1) replenishment of water resources across the
184 Chinese arid region is mainly from melted glacial or perennially ly frozen soil, but not
185 from precipitation; (2) meteorological observations in the arid regions of China~~Chinese~~
186 ~~arid regions~~ are too scarce to conduct robust analysis (Wu et al., 2007; Xu et al., 2015);
187 (3) from a practical perspective, calculating climate extreme indices across arid region
188 ~~with large-scale~~and ~~desert~~ ~~region~~ is less meaningful~~less~~ (Tomas-Burguera et al., 2020).

189 ~~The two commonly used indices (i.e., monthly Palmer drought severity index (PDSI)~~
190 ~~and standardized precipitation evapotranspiration index (SPEI) were employed for~~
191 ~~comparison. PDSI and SPEI were computed from the same meteorological data~~
192 ~~described above. The conventional PDSI was empirically derived using the~~
193 ~~meteorological data of the central USA with its semi-arid climate. The portability of~~
194 ~~the conventional PDSI is thus relatively poor (Liu et al., 2017). In this study, PDSI was~~
195 ~~calculated according to the China national standard of classification of meteorological~~
196 ~~drought with standard number of GB/T 20481-2017. The PDSI was built based on long-~~
197 ~~term meteorological data of in-situ stations evenly distributed around China, hence well~~

198 ~~monitor drought in China (Zhong et al., 2019a), and the detailed calculation on the~~
199 ~~PDSI is shown in supplementary materials.~~ The 0.25°-daily root zone (0 - 100 cm) soil
200 moisture dataset obtained from [the](#) Community Land Model of the Global Land Data
201 Assimilation System ([Li et al., 2018; Rodell et al., 2004](#)) was also used in this study.
202 [The](#) Community Land Model product does not have explicit vertical levels, instead soil
203 moisture is represented in surface (0-2cm), and root zone [soil moisture](#) (0-100cm) ([Li](#)
204 [et al., 2018](#)). Root zone soil moisture is chosen over the surface soil moisture on account
205 of its ~~appropriateness~~ ~~esiteness~~ to characterize drought ~~and~~; lower noise relative to
206 surface soil moisture (Hunt et al., 2009; Osman et al., 2020). The dataset from 1961 to
207 2014 were downloaded from the Goddard Earth Sciences Data and Information
208 Services Center (<https://earthdata.nasa.gov/eosdis/daacs/gesdisc>~~Rodell et al., 2004~~).
209 The soil moisture dataset from [the](#) Community Land Model ~~can well~~ captures dry and
210 wet conditions in China well (Bi et al., 2016; Feng et al., 2016). To avoid the effect of
211 seasonality, ~~the~~ soil moisture was fitted by [a](#) Gamma ~~probability~~ distribution, and ~~then~~
212 ~~was~~ ~~subsequently~~ standardized by normal quantile transformation ([Herr and](#)
213 [Krzysztofowicz, 2005](#)). ~~In addition, 8-day leaf area index of the MOD15A2H from~~
214 2003 to 2018 were collected. ~~These data were~~ ~~After resampled~~ ~~resampling~~ to [a](#) 0.25°
215 spatial resolution, ~~we subtracted the local mean and divided by the local standard~~
216 ~~deviation, and then the Z-score was used~~ to ~~calculate the~~ [obtain normalized](#) leaf area
217 index anomalies.

218 We further used ~~eight~~ global climate models ~~s~~ from the Coupled Model
219 Intercomparison Project Phase 5 (<https://esgf.llnl.gov/>) [to assess the effect of climate](#)
220 [model biases on compound dry-hot events](#) (~~Taylor et al., 2012~~), ([Taylor et al., 2012](#)).
221 ~~including~~ [The global climate models used in this study include](#) CanESM2, CNRM-
222 CM5, CSIRO-Mk3.6, MIROC-ESM, MPI-ESM-LR, BCC-CSM1-1, IPSL-CM5A-LR,

223 and MRI-CGCM3₁, ~~were used to project the future climate conditions.~~ These global
224 ~~climate~~ models exhibit good performance ~~to~~ in their simulate simulation of the key
225 features of precipitation and temperature in China (Jiang et al., 2016; Yang et al., 2019).
226 We obtained daily climate variables (e.g., precipitation, temperature, relatively
227 humidity, and wind speed) for the historical (1961-2005) ~~future (2050-2100)~~ periods,
228 ~~for the three Representative Concentration Pathways (RCPs) including RCP 2.6 (low~~
229 ~~emission scenario), RCP 4.5 (moderate emission scenario) and RCP 8.5 (high emission~~
230 ~~scenario).~~ All of the global climate models' outputs were based on the first ensemble
231 member of each model, ~~referred to as r1i1p1 in all of the experiments.~~ In this study,
232 the bias-corrected climate imprint method, one of the delta statistical downscaling
233 methods, was used to downscale the global climate models outputs to a spatial
234 resolution of 0.25° (Werner and Cannon, 2016). The detailed information on these
235 global climate models is shown in Table S1.

236 **2.2 Development of SCDHI**

237 The SCDHI is a compound drought and heat index based on a daily drought index
238 and the STI, both of which are briefly introduced in the following, ~~which is computed~~
239 ~~in a similar fashion as the Standardized Precipitation Index (Zscheischler et al., 2014).~~
240 ~~The calculation of daily STI is similar to monthly STI, but for standardizing daily~~
241 ~~temperature. For example, with respect to one certain grid point, the 1 January STI are~~
242 ~~computed on the 1 January temperature datasets observed during 1961-2018 at each~~
243 ~~grid point. We firstly formulated~~ The STI and a daily scale drought index, i.e., the
244 SAPEI will be quickly introduced in the following i.e. the SAPEI, by considering both
245 ~~precipitation and potential evapotranspiration. The Penman Monteith method is used~~
246 ~~to calculate the potential evapotranspiration. Afterward, the~~ Afterwards, we will
247 explain how the joint distribution method was employed to compute the SCDHI from

248 [the two univariate indices](#).

249 **2.2.1 Formulation of daily-scale drought [and heat index](#) indices**

250 ~~Li et al. (2020b) have proposed the daily scale drought index (SAPEI) that~~
251 ~~considers both precipitation and potential evapotranspiration. H~~[The daily-scale drought](#)
252 [index \(SAPEI\) was first introduced by Li et al. \(2020b\). H](#)However, the primary
253 limitation of this index is that it has a fixed temporal scale ([the number of considered](#)
254 [antecedent days was equal to 100](#)) and cannot reflect ~~the~~ dry and wet condition at
255 different time scales. [Given that drought is a multi-scalar phenomenon \(Mckee et al.,](#)
256 [1993, Vicente-Serrano et al., 2010\), here we extended the SAPEI to a multiple time](#)
257 [scale \(i.e., 3-, 6-, 9-, and 12-month\) daily drought index. Hence, we developed the](#)
258 [multiple time scale \(i.e., 3-, 6-, 9-, and 12-month\) daily drought index. Hence, in this](#)
259 ~~study, we developed the multiple time scale (i.e., 3-, 6-, 9-, and 12-month) daily drought~~
260 ~~index. Here, we followed the same nomenclature proposed by Li et al. (2020b) to refer~~
261 ~~to a daily standardized drought index (SAPEI) based on precipitation and potential~~
262 ~~evapotranspiration. SAPEI is simple to calculate, and uses the antecedent accumulative~~
263 ~~differences between precipitation and potential evapotranspiration to represent the dry~~
264 ~~and wet condition of the current day. The calculation procedure is described below.~~

265 The Penman-Monteith method (Allen et al., 1998) was ~~firstly~~ used to compute
266 potential evapotranspiration. ~~With a value for potential evapotranspiration, t~~[The daily](#)
267 difference between precipitation and potential evapotranspiration was [then](#) calculated
268 to ~~reveal~~ [estimate](#) ~~climatic~~ [the](#) water balance. ~~(precipitation minus potential~~
269 ~~evapotranspiration)~~. To reflect dry and wet conditions of ~~the~~ [a given](#) day, the antecedent
270 water surplus or deficit (WSD) was calculated through the following equations:

$$WSD = \sum_{i=1}^n (P - PET)_i \quad (1)$$

271 ~~w~~Where n is the number of previous days, PET represents the potential
 272 evapotranspiration, and P represents precipitation.

273 The WSD values can be aggregated at different time scales, such as 3, 6, 9 months, and
 274 so on. The daily WSD series was fit to a log-logistic distribution. Subsequently,
 275 cumulative probabilities of the WSD series were obtained and transformed to
 276 standardized units using the classical approach of Barton et al. (1965), resulting in the
 277 SAPEI.

278 The STI was computed in a similar fashion as the SPI, while it did not accumulate
 279 temperature in a fixed scale. The calculation of daily STI relied on daily temperature.
 280 A normal distribution was fitted to daily temperature at each day of the year, because
 281 temperature anomalies can be assumed to be normally distributed (Hansen et al., 2012;
 282 Zscheischler et al., 2014). The STI was then computed based on the cumulative
 283 distribution function $G(x)$, that is, are listed below:

$$G(x) = \frac{1}{\sigma\sqrt{2\pi}} \int_{-\infty}^x \exp\left(-\frac{(x-\mu)^2}{2\sigma^2}\right) dx \quad (2)$$

$$STI = \varphi^{-1}(q) \quad (3)$$

284 where x is temperature time series. x and σ are the mean and standard deviation
 285 parameters, respectively. q is the cumulative probability and φ is the standard normal
 286 distribution.

287 ~~A probability distribution was used to fit the daily time series WSD. Given that different~~
 288 ~~probability distributions may cause differences in drought indices (Stagge et al., 2015),~~
 289 ~~to select the most suitable distribution, several commonly probability distributions~~

290 including the general extreme value, log-logistic, lognormal, Pearson III, generalized
291 Pareto, exponential, and normal distributions, should be used to fit the WSD series. In
292 the study of Li et al. (2020b), Shapiro-Wilk and Kolmogorov-Smirnov test have been
293 used applied for optimal probability distribution selection by comparing the empirical
294 probability distribution with a candidate theoretical probability distribution. They
295 suggested that the log-logistic distribution is more suitable for SAPEI. Moreover,
296 previous researches have demonstrated that the log-logistic distribution is suitable for
297 standardizing drought indices, e.g. SPEI (Vicente-Serrano et al., 2010). Therefore, we
298 chose the log-logistic distribution to compute SAPEI. Once the daily WSD series were
299 fit to a probability distribution, cumulative probabilities of the WSD series were
300 obtained and transformed to standardized units (SAPEI) using the classical approach of
301 Barton et al. (1965).

302 2.2.2 Construction of SCDHI

303 The SCDHI was established ~~through~~ using copula theory (a brief introduction on
304 copula theory is ~~shown~~ given in supplementary materials), which ~~can~~ essentially
305 ~~combine models~~ the candidate variables into one numerical expression dependence
306 between the SAPEI and the STI to generate a bivariate distribution linking the two
307 indices. ~~This approach not only realizes a projection from multiple dimensions to a~~
308 ~~single dimension, but also the marginal distributions of the candidate variables~~
309 ~~combined with their original structures can be fully preserved within the constructed~~
310 ~~joint distribution. Hence, the copula-based index provides an objective description of~~
311 ~~the compound events (Hao et al., 2018b; Terzi et al., 2019).~~

312 There are many copula families available, which have widely been used for jointing
313 modelling bivariate distributions (Terzi et al., 2019). Among ~~then~~ them, Clayton,
314 Gumbel, Normal, t, and Frank copula perform well for jointing bivariate

315 hydrometeorological variables (Ayantobo et al., 2018; Liu et al., 2019), and thus were
 316 ~~employed~~ tested to establish the bivariate joint probability distribution in this study.
 317 Assuming, the two random ~~Gaussian~~ variables X and Y , representing SAPEI and STI,
 318 respectively, the compound dry-hot event can be identified as one variable X ~~lower~~
 319 less than or equal to a threshold x , and the other variable Y higher than a threshold y
 320 at the same time. The joint probability P of the compound dry-hot event can then be
 321 expressed as:

$$p = P(X \leq x, Y \geq y) = u - c(u, v) \quad (24)$$

322 where u ~~and~~ v are ~~was~~ the respective thresholds after transforming X and Y to
 323 uniform marginal distributions (Ayantobo et al., 2017), ~~respectively~~, and $c(u, v)$ ~~was~~ is
 324 the joint probability distribution based on the fitted copula (Zscheischler and
 325 Seneviratne, 2017a).

326 This joint cumulative probability P ~~could~~ can then be treated as an indicator, where
 327 smaller P values denote more severe condition of compound dry-hot ~~event~~ conditions.
 328 ~~However, P to the given marginal sets, P values in different seasons or areas~~
 329 ~~reflected different conditions and are thus not comparable.~~ However, because the
 330 marginal distributions usually vary across seasons and regions, the same value of does
 331 not correspond to the same univariate exceedance thresholds across seasons and regions
 332 but rather refer to similar bivariate extremeness in the bivariate SAPEI-STI distribution.
 333 ~~Hence,~~ Transforming the joint probability P ~~was transformed in~~ to a uniform

334 distribution by fitting a distribution F , and subsequently into a standard normal
335 distribution results in~~which was then standardized as~~ an indicator to characterize
336 compound dry-hot events. ~~Once the P -series at each day were fitted to a copula, the P -~~
337 ~~series were transformed to standardized units.~~Hence, the SCDHI ~~can be estimated~~is
338 computed by taking the inverse of the joint cumulative probability (p)-~~as~~:

$$SCDHI = \varphi^{-1}(F(P(X \leq x, Y \geq y))) \quad (35)$$

339 where φ is the standard normal distribution function and, F is the marginal
340 cumulative distribution, which remaps the joint probability to the uniform distribution
341 (Yeo and Johnson, 2000).~~the distribution F was estimated based on the Yeo-Johnson~~
342 ~~transformation formula (Yeo and Johnson, 2000).~~

343 Following the categories of compound dry and hot conditions as suggested by Wu
344 et al. (2020) ~~(Wu et al., 2020)~~, we defined ~~five~~ five categories of compound dry and hot
345 conditions, including abnormal, light, moderate, heavy and extreme compound
346 ~~drought~~dry-hot, as shown in Table 1. The development of the SCDHI is illustrated in
347 Fig. 2.

348 ~~We used Akaike information criterion, Bayesian information Criterion, and~~
349 ~~Kolmogorov-Smirnov statistics as goodness-of-fit measures to select an appropriate~~
350 ~~copula. These statistical measures have been commonly used for estimating the~~
351 ~~goodness of fit of a proposed cumulative distribution function to a given empirical~~
352 ~~distribution function (Liu et al., 2019; Terzi et al., 2019). The statistics of the three~~
353 ~~metrics are presented in Fig. S1-3. According to the evaluation metrics, the Frank~~
354 ~~copula was utilized to establish the joint probability function and construct SCDHI in~~
355 ~~this study. Note that the SCDHI under three future scenarios is also used the Frank~~
356 ~~copula, while the parameters are assessed by future scenarios data. The SCDHI~~

357 development was illustrated in Fig. S4.

358 Furthermore, to verify the ability of SCDHI to capture the compound dry and hot
359 event, three verification metrics were used (i.e., probability of detection, false alarm
360 ratio, and critical success index) (Winston and Ruthi, 1986).

$$\text{Probability of detection} = \text{hit} / (\text{hit} + \text{miss}) \quad (4)$$

$$\text{False alarm ratio} = \text{false alarm} / (\text{hit} + \text{false alarm}) \quad (5)$$

$$\text{Critical success index} = \text{hit} / (\text{hit} + \text{false alarm} + \text{miss}) \quad (6)$$

361 where *hit* (observed drought hot) refers to the number of grids when SAPEI and
362 STI is subjected to grade 1-4 and SCDHI is subjected to grade 1-4; *Miss* denotes the
363 number of grids when SAPEI and STI is between grade 1-4 and SCDHI is subjected to
364 other grades than grade 1-4; *False alarm* denotes the number of grids when SAPEI and
365 STI is subjected to other grades than grade 1-4 but SCDHI is subjected to grades of
366 grade 1-4.

367 2.2.3 Evaluation metrics

368 We used the Akaike information criterion (AIC), Bayesian information Criterion
369 (BIC), and Kolmogorov-Smirnov (KS) statistics to select the most appropriate copula.
370 The KS test indicates the goodness-of-fit between the empirical and theoretical
371 distributions (Wu et al., 2018), while the BIC and AIC are a relative measure of the
372 quality of a model for a given set of data and helps in model selection among a finite
373 set of models (Li et al., 2013). The preferred model is the one with the lower AIC and
374 BIC values but the higher p values in the KS test. These statistical measures have been
375 commonly used for selecting appropriate copulas (Zscheischler et al., 2017;
376 Zscheischler and Seneviratne, 2017; Liu et al., 2019; Terzi et al., 2019). The statistics

377 of the three metrics are presented in Fig. S1-3, indicating that the Frank copula showed
378 lower AIC and BIC values but higher p values of KS test compared to other copulas.
379 Overall, all test showed comparable results. The Frank copula was thus utilized to
380 model the dependence between SAPEI and STI and to construct the SCDHI as
381 explained in Section 2.2.2. ~~Note that for the SCDHI under three future scenarios we~~
382 ~~also used the Frank copula, refitting the parameters to the data from the climate model~~
383 ~~projections.~~

384 **2.3 Other drought indicators**

385 The two commonly used drought indices monthly Palmer drought severity index
386 (PDSI) and standardized precipitation evapotranspiration index (SPEI) were employed
387 for comparison against SAPEI. The conventional PDSI was empirically derived using
388 the meteorological data of the central USA with its semi-arid climate. The portability
389 of the conventional PDSI to other world regions is thus relatively poor (Liu et al., 2017).
390 In this study, PDSI was calculated according to the China national standard of
391 classification of meteorological drought with standard number of GB/T 20481-2017.
392 The PDSI was built based on long-term meteorological data of in-situ stations evenly
393 distributed around China (Zhong et al., 2019a). The detailed calculation on the PDSI
394 and SPEI are presented in the supplementary materials.

395 **2.4 Run theory to extract compound event characteristics**

396 Run theory (Yevjevich and Ingenieur, 1967) was used to identify the frequency,
397 duration, severity, and intensity of compound dry-hot events. A ‘run’ is defined as a
398 portion of the time series of a variable X_t , in which all values are either below (i.e.,
399 negative run) or above (i.e., positive run) a selected truncation level of X_0 (Ayantobo

et al., 2017). Figure 3 illustrates an example with two compound dry-hot events, and each compound dry-hot event is characterized by its respective duration, severity, intensity, and non-compound dry-hot condition. Specifically, according to the truncation level X_0 , the number of consecutive intervals (days) where values remain below X_0 defines *duration*, while the cumulative sum of values during a compound dry-hot period and the minimum value within a compound dry-hot period defines *severity* and *intensity*, respectively. *Frequency* is simply the number of events in the given time period. Duration and severity are thus defined as:

$$\underline{duration} = t_e - t_i \quad (12)$$

$$\underline{severity} = \sum_{t=1}^D SCDHI_t \quad (13)$$

where t_e is terminate time, t_i is initiation time, D is duration. In this study, X_0 was set to -0.8, -1.3, and -1.6 to assess the characteristics of compound dry-hot events under different thresholds. Furthermore, for the assessment of compound event characteristics in this study, events shorter than two weeks were discarded.

3 Results and ~~Discussion~~discussion

3.1 Evaluation of SAPEI

The SCDHI was established based on the daily STI and the daily-scale drought index, ~~i.e.~~, SAPEI. However, no previous studies have tested the daily drought monitoring performance of the SAPEI at multiple time scales. ~~When developing a drought index, rigorous testing is required with respect to its applicability before it is applied in drought monitoring.~~ Figure 2-4 shows the spatial distributions and probability density densities of the correlations between SAPEI and SPEI/PDSI/soil moisture across China. The monthly mean SAPEI at 3-, 6-, 9- and 12-month scale all ~~showed~~ shows strong agreement with the SPEI in China, and, ~~with~~ correlation

423 coefficients were typically higher than 0.8 ($p < 0.01$), indicating that the monthly
424 SAPEI at multiple time scale calculated from ~~the~~ daily values could have the same
425 similar capability to monitor monthly drought as SAPEI. ~~of monthly drought monitoring~~
426 ~~as SPEI~~. The 3-, 6-, 9- and 12-month SAPEI also generally showed ~~good~~ high
427 correlations with the PDSI, ~~and in particular the~~ 3-month SAPEI and PDSI are
428 well generally correlated d ~~closely~~, with correlation coefficients higher than 0.6 ($p < 0.01$).
429 For the daily SAPEI at 12-month scale and soil moisture, a close correlation was
430 detected in south and north China, while relatively weak correlation ~~is~~ was found in
431 Midwest China. The correlation between SAPEI and soil moisture increased in
432 magnitude at time scales of 3 to -9 months. For the 12-month SAPEI, mean correlation
433 coefficient reached about 0.5 for ~~whole~~ all of China. ~~The~~ is ~~phenomenon implied results~~
434 indicate that the short-time scale SAPEI ~~was~~ is more sensitive to precipitation
435 ~~change~~ variability, and thus could be more suitable for meteorological drought, while
436 the long-time scale (more than five month) SAPEI ~~was~~ is more closely related to soil
437 moisture and can thus be applied for agricultural drought monitoring. Overall, these
438 analyses indicate that the SAPEI at daily and monthly scale ~~showed reliability~~ is a
439 reliable indicator ~~in for~~ drought monitoring at different time scales.

440 To further test the drought monitoring performance of the SAPEI, typical drought
441 events were chosen as case studies. ~~During recent decades, several well-known large-~~
442 ~~scale drought events have hit China, including the droughts in winter of 2009 to spring~~
443 ~~of 2010, and in 2011 (Lu et al., 2014; Yu et al., 2019). In this study, the drought regimes~~
444 ~~during these events were taken as case studies to evaluate the drought monitoring~~
445 ~~performance of SAPEI at 3-month time scales (Sun and Yang, 2012).~~ We firstly showed
446 the monthly evolution of these events by the monthly mean SAPEI, SPEI, and PDSI,
447 and then analyzed the temporal ~~daily~~ evolution of drought at daily scale ~~in space and~~

448 ~~time~~ in the most affected areas according to SAPEI and soil moisture.

449 **3.2.1 Drought events during 2009-2010**

450 ~~As shown in Fig. S5, the monthly evolution in 2009/10 drought based on SAPEI~~
451 ~~was generally similar with that of SPEI and PDSI. This drought started to appear in~~
452 ~~most of China (except for the central and northeast China) in September 2009, and then~~
453 ~~persisted in most of China during October to December 2009. During January and April~~
454 ~~in 2010, severe drought persisted in southwest China, while drought in the rest of China~~
455 ~~gradually disappeared in this period. After that, dry conditions in southwest China~~
456 ~~gradually relieved from May to June in 2010, but did not disappear.~~

457 Despite being located in the humid climate zone, southwest China suffered from
458 exceptional drought during the autumn of 2009 to the spring of 2010 (Lin et al., 2015).

459 ~~During this drought, more than 16 million people and 11 million livestock faced~~
460 ~~drinking water shortages, with direct economic losses estimated at 19 billion yuan in~~
461 ~~southwest China (Lin et al., 2015). We selected this event in southwest China as the~~
462 ~~first case study, and reveal spatial and temporal change of this event at daily scale based~~
463 ~~on SAPEI and soil moisture (Fig. 3 and 4). We selected this event in southwest China~~
464 as the first case study. As shown in Fig. S4, the monthly evolution in 2009/10 drought
465 based on SAPEI was generally similar with that of SPEI and PDSI. Figure 5 reveals the
466 daily change of this event using SAPEI and soil moisture. During ~~the~~ September ~~1 to~~
467 ~~30~~ of 2009, the drought started to appear in the region, and dry conditions became worse
468 and spread throughout nearly the entire southwest of China from October 1 to
469 November 15 of 2009. Severe dry conditions then stayed in the region for 152 days
470 from November 15 to April 15 of 2010, with high intensity. Afterwards, severe drought
471 was gradually relieved from April 15 to June 15. The drought diminished over time in
472 most parts of southwest China by the end of June.

3.2.2 Drought events in 2011

As shown in Fig. S6, the 2011 drought monthly pattern monitored by SAPEI are generally consistent with those by SPEI and PDSI. The drought mainly started in north China in January, while in March it spread to most of China, and severe dry conditions persisted in most areas during April to May. In August, the drought mainly moved to southward. Severe drought persisted in southwest China during September and October, but it then gradually faded away. The results monitored by the SAPEI are generally consistent with the findings of Lu et al. (2014).

In 2011, a particularly unusual drought event was particularly unusual occurred in the middle and lower reaches of the Yangtze River Basin (MLR-YRB). The MLR-YRB is generally in a wet condition, nevertheless, it suffered its worst drought in the recent 50 years during the spring 2011. The severe drought caused shortage of drinking water for 4.2 million people and 3.7 million hectares of crops were damaged or destroyed (Lu et al., 2014; Xu et al., 2015). Moreover, the heavy drought led to more than 1,300 lakes devoid of all water in Hubei province (Xu et al., 2015). The temporal and spatial evolution of this event in MLR-YRB described by daily SAPEI and soil moisture was shown in Fig. 5-6. As shown in Fig. S5, the monthly spatial evolution of the 2011 drought indicated by the SAPEI are broadly similar to those by SPEI and PDSI. The temporal evolution of this event in MLR-YRB described by daily SAPEI and soil moisture is shown in Fig. 6. The drought started to appear in the northern part of the MLR-YRB in early February of 2011, and then gradually expanded to the whole MLR-YRB during early February and until March 15. The severe drought condition persisted in this region for 78 days (from March 15 to May 31). Afterwards, there was a tendency toward alleviating drought conditions alleviated, and most of MLR-YRB was continued to be under light and moderate drought

498 conditions.

499 Overall, similar to the SPEI, SAPEI includes multiple time scales (3-, 6-, 9-, and
500 12- month) to monitor drought at monthly resolution and is relatively sensitive to soil
501 moisture variations. However, the SAPEI has the advantage to allow for sub-monthly
502 drought monitoring. Such an index could help fill a gap between science and
503 applications in that it could be operationally used for detecting and monitoring both
504 short-term and persistent droughts.

505 ~~The previous detailed analysis showed that the SAPEI not only captures monthly~~
506 ~~characteristics of droughts, but also has the potential to track droughts at sub-monthly~~
507 ~~scale (Li et al., 2020b). Though the input data (including precipitation and potential~~
508 ~~evapotranspiration) of SAPEI are similar to SPEI, the rationale of the index is different~~
509 ~~from SPEI. It was calculated for each day and considers the water surplus or deficit of~~
510 ~~that day and the previous days. SPEI was commonly employed to monitor and analyze~~
511 ~~the monthly or longer scale droughts (Vicente Serrano et al., 2010). It thus may not be~~
512 ~~appropriate to apply the SPEI at shorter timescales (e.g., daily or weekly), because of~~
513 ~~the inherent problem in the construction of the index. Although SPEI gives a full and~~
514 ~~equal consideration to the water surplus or deficit in the period of the considered time~~
515 ~~scale, it does not consider the water surplus or deficit in the days before the period. If~~
516 ~~the scale is very short, this may cause problems. For a 7-day period, for example, if~~
517 ~~there is no precipitation during the period, it may be regarded as a drought period when~~
518 ~~compared with historical records (the method used by the SPEI); however, if there is a~~
519 ~~heavy precipitation just before the period, then the 7-day period probably remains wet~~
520 ~~and is unlikely to experience drought condition during such a short time. Previous~~
521 ~~studies have demonstrated the disadvantage of SPEI for short-time scale drought~~
522 ~~monitoring (Lu, 2009; Lu et al., 2014; Li et al., 2020b).~~

523 ~~Soil moisture would be the most appropriate variable for agriculture drought~~
524 ~~monitoring and analyses (Mishra and Singh, 2010). However, there are few long-term~~
525 ~~and large-scale observational soil moisture datasets due to insufficient observation~~
526 ~~stations around the world, especially for developing regions, which limits its wide use~~
527 ~~in drought monitoring and analyses (Seneviratne et al., 2010). Thus, using~~
528 ~~observational hydrometeorological datasets, the complex physical process models, such~~
529 ~~as the variable infiltration capacity model, are widely used to simulate the soil moisture~~
530 ~~(Liang et al., 1996; Xia et al., 2018). However, running such models requires highly~~
531 ~~trained personnel not usually available at local agencies. In addition, when the model~~
532 ~~is used locally, it generally needs to be calibrated and verified by observational datasets~~
533 ~~(Xia et al., 2018; Zhou et al., 2019). This certainly limits the wide use of soil moisture~~
534 ~~as a drought indicator.~~

535 ~~In summary, the SAPEI meets the requirements of a drought index, given the fact that~~
536 ~~it shows reliable and robust ability for drought analysis and monitoring. Like the SPEI,~~
537 ~~SAPEI includes multiple time scales (3-, 6-, 9-, and 12-month) to monitor drought at~~
538 ~~monthly resolution and is relatively sensitive to soil moisture variation. However,~~
539 ~~SAPEI has the advantage over SPEI regarding sub-monthly drought monitoring. Such~~
540 ~~an index could help fill a gap between science and applications in that it would be~~
541 ~~operationally tractable for detecting and monitoring both short-term and sustained~~
542 ~~droughts.~~

543 **3.2 Evaluation of the SCDHI**

544 The SCDHI was developed by ~~joining-linking~~ the marginal distribution of the
545 SAPEI and STI. Though the copula method has been widely utilized to connect
546 ~~bivariate two dependent~~ distributions, the ~~property-ability~~ of the SCDHI ~~to~~ in capturing
547 capture compound dry-hot events ~~still~~ needs to be tested. Figure 7 shows the spatial

548 distributions of the correlations between SCDHI and SAPEI/STI at daily scale across
549 China. The SCDHI all showed strong ($p < 0.01$) correlation with the SAPEI at 3-, 6-,
550 9- and 12-month scale in China, with correlation coefficients higher than 0.7. A
551 significant correlation ($p < 0.01$) was also detected between STI and SCDHI at multiple
552 ~~Fig. 7 shows the spatial pattern and density for probability of detection, false~~
553 ~~alarm ratio, and critical success index when the drought and hot events observed~~
554 ~~identified by the SAPEI and STI, respectively were related toin relation to compound~~
555 ~~drought hot events detected by SCDHI at 3-, 6-, 9- and 12- monthly scale. As shown in~~
556 ~~Fig. 7, pProbability of detection is close to 1 and false alarm ratio is close to 0, implying~~
557 ~~that SCDHI can well detect in most of the areas where the droughts and hot extremess~~
558 ~~were detected by SAPEI and STI. The values of the critical success index indicated that~~
559 ~~the ratios of drought hot affected areas locations where compound droughts and hot~~
560 ~~extremes were detected by SAPEI and STI to the ones drought and hot areas detected~~
561 ~~by the SCDHI were close to one. Hence, overall the SCDHI is well correlated with~~
562 univariate variations in drought and heatwave occurrence.~~Overall, these analyses~~
563 ~~implied that SCDHI can well monitor droughts and hots that can be successfully~~
564 ~~captured by SAPEI and STI. The SCDHI thus detects compound dry hot events that are~~
565 ~~identified separately by the coincidence of low SAPEI and high STI. In addition, the~~
566 ~~SCDHI detects events that are very extreme in either the SAPEI or the STI can and~~
567 ~~moderate in the other variable but thus still cause substantial damage (Zscheischler et~~
568 ~~al., 2017b). Furthermore, as a univariate indicator, the SCDHI is able to quantify the~~
569 ~~magnitude of compound dry hot events.~~

570 To further test the drought-heat monitoring performance of the SCDHI, two typical
571 compound dry-hot events were chosen as case studies according to the Yearbook of
572 Meteorological Disasters in China. One ~~was~~ is a well-known compound drought and

573 heatwave striking Sichuan-Chongqing region with serious consequences during
574 summer of 2006 (Wu et al., 2020), and the other occurred in southern China with
575 adverse impacts on agriculture during July to September of 2009 (Wang et al., 2010).
576 The Sichuan-Chongqing region experienced continuous extreme temperatures during
577 mid-June to late August 2006. The duration and severity of this ~~hot event~~heatwave were
578 the worst on the historical record. Simultaneously, a ~~heavy 100-year~~ drought ~~occurring~~
579 ~~once in 100 years~~ hit ~~this~~ the region. During this compound event, a population of over
580 ten million was confronted with drinking water shortage, about ~~twenty thousand~~ 20,000
581 km² of cropland suffered serious losses, and more than one hundred ~~times~~ forest fires
582 broke out. Local governments issued the most serious aridity warning (Zhang et al.,
583 2008). ~~Thus, we take this typical drought hot event as first case study studies to evaluate~~
584 ~~the drought/hot monitoring performance of SCDHI.~~ The monthly spatial pattern of this
585 compound event in the Sichuan-Chongqing region is shown in Fig. ~~S7S6~~, indicating
586 that ~~Sichuan-Chongqing~~the region ~~during summer in 2006~~ experienced ~~the~~ moderate to
587 extreme compound dry and hot conditions based on the SCDHI during the 2006
588 summer. Fig-~~ure~~ 8 maps the spatial pattern of this compound event and its impact on
589 vegetation from mid-June to late August at weekly scale. ~~This~~ The event started to
590 appear in the Sichuan-Chongqing region in mid-June 2006, and gradually spread
591 throughout the whole Sichuan-Chongqing region during June 19 to 26. The moderate
592 dry-hot conditions then persisted in the entire Sichuan-Chongqing region from June 27
593 to August 5 ~~in~~ 2006, lasting for 40 days. ~~The~~ Scattered negative leaf area index ~~was~~
594 ~~scattered~~ appeared in some of the dry-hot affected areas. ~~However,~~ during August 6
595 to 21, the ~~drought~~ dry-hot event became ~~even~~ more severe with the onset of extremely
596 hot temperatures, causing negative vegetation anomalies in most of the affected areas.

597 The monthly spatial patterns of another compound event in southern China during

598 July to September of 2009 ~~is~~are shown in Fig. ~~S8~~S7. Overall moderate to heavy
599 compound dry and hot conditions are observed at monthly scale in this region. However,
600 ~~this~~the event showed large fluctuation at weekly scale. According to the Yearbook, the
601 ~~hot event~~heatwave was divided into two periods: the first stage was from early to late
602 July, and the other stage was from mid-August to early September. The fluctuating
603 compound event caused adverse impacts ~~of~~on crop pollination and grain filling,
604 resulting in decrease ~~of~~d crop production. Fig. ~~ure~~9 maps the spatial pattern of this
605 event and its impact on the leaf area index at weekly scale. In the first stage, the
606 ~~drought~~dry-hot event hit ~~the~~ most of southern China during July 5 to 12, ~~and then~~before
607 it became more severe in the western part of southern China during July 13 to 20.
608 ~~However,~~ ~~t~~The ~~hot event~~heatwave suddenly disappeared ~~from~~between July 21 to 28,
609 leading to disappearance of the compound event in most of southern China (Fig. 9a).
610 ~~Afterward~~Afterward, the compound event hit this region again from August 6 to 13,
611 and its intensity was particularly strong during August 14 to 21, with ~~severe~~very hot
612 conditions. Subsequently, the intensity and spatial extent of the compound event faded
613 away in the north of southern China during August 22 to 29. This event extended to
614 most of this region again from August 30 to September 14, with severe dry and hot
615 conditions. The compound events still stayed in this region from September 15 to 22
616 (Fig. 9b). Despite the short-term event, ~~the~~anormal ~~changer~~reductions in vegetation
617 activity ~~was~~were found in most of the dry-hot affected areas. This complex event
618 indicates that monthly analyses of ~~the~~compound events ~~can~~ provide an overall
619 situation, but ~~is~~are ~~unnot~~be able to capture the serious compound dry and hot
620 conditions caused by ~~a short-term~~ extreme climate ~~anomaly~~anomalies at shorter time
621 scales. ~~Though such short-term compound~~ ~~dry-hot events~~ ~~only lasted~~ ~~last~~ ~~for days or~~
622 ~~weeks,~~ such events they can lead to large agricultural losses if they occur within the

623 ~~sensitive stages inof crop development (i.e.e.g., pollination and grain filling)~~
624 ~~(Mazdiyasni and AghaKouchak, 2015). To provide timely information of the~~
625 ~~compound dry hot events, short time scale analyses and monitoring of such events are~~
626 ~~essential.~~

627 Overall, the changes in these two compound dry-hot events based on [the](#) SCDHI
628 are consistent with the national weather records (<http://www.weather.com.cn/zt/kpzt/>)
629 and the Yearbook of Meteorological Disasters in China 2010. In summary, the SCDHI
630 is able to robustly and reliably capture compound dry-hot events at sub-monthly scale,
631 and potentially provide a new tool to objectively and quantitatively analyze and monitor
632 the characteristics of compound dry-hot events in time and space.

633 **3.3 Application [of the SCDHI in China](#)**

634 ~~Here, w~~[We](#) ~~evaluated~~ and ~~compared~~ the spatiotemporal variation of characteristics
635 of compound dry-hot events in China during [the](#) growing season (April-September),
636 because such events can more easily cause adverse impact on agriculture and ecosystem
637 during these periods (Hao et al., 2018; Wu et al., 2019; [Zscheischler & Fischer, 2020](#)).
638 ~~More precisely, the compound dry hot events from 1961 to 2018~~ [More precisely, the](#)
639 [compound dry-hot events and their characteristics \(frequency, duration, severity, and](#)
640 [intensity\)](#) were identified based on 3-month scale SCDHI and run theory ~~at~~[with](#)
641 [different thresholds](#) (Wu et al., 2018). [We further assessed how well climate models are](#)
642 [able to represent compound event characteristics.](#), ~~after which the frequency, duration,~~
643 ~~severity, and intensity of these events were analyzed (A specific case to identify~~
644 ~~compound dry hot event is shown in Fig. S9). We then projected their future~~
645 ~~characteristics changes under the RCP 2.6, 4.5 and 8.5 from 2050 to 2100.~~ Given that
646 short-term concurrent dry and hot events ~~generally~~ [often](#) persist for at least weeks
647 (Otkin et al., 2018), only ~~the~~ events [that lasting lasted](#) for more than two weeks ~~were~~

648 are considered ~~in this study~~.

649 Fig. ~~ure 9-10~~ shows spatial patterns of key characteristics of the identified
650 compound dry-hot events with the threshold being set to -0.8 in run theory. A high
651 frequency of compound events ~~was~~ is detected in southern China, with occurrence of
652 one event every two years on average, ~~in~~ In contrast, the eastern Tibetan Plateau and
653 northeast China experienced fewer compound events (Fig. 10a), which was generally
654 consistent with ~~the earlier previous~~ studies (Liu et al., 2020; Wang et al., 2016). On
655 average, The compound dry-hot events generally lasted for about ~~twenty20-five~~ to
656 ~~thirty-five~~ 35 days in most of China, while in the eastern Tibetan Plateau, ~~the~~ compound
657 dry-hot event persisted for less than twenty days (Fig. 10b). ~~The~~ Mean severity and
658 intensity of ~~the~~ compound dry-hot event ~~presented relatively~~ show somewhat similar
659 patterns in relative terms and ~~showed~~ highlight that most of eastern China experienced
660 the highest severity and intensity (Fig. 10c-d). The spatial patterns are overall similar
661 when using a threshold of -1.3 (Fig. 11) of -1.6 (Fig. S8) in run theory. As expected,
662 frequency and duration tend to decrease, while severity stays similar and intensity tends
663 to increase at more extreme thresholds. White areas indicate regions where no events
664 longer than two weeks occurred.

665 ~~Overall, southern China suffered~~ suffers more frequent compound dry-hot events,
666 with higher severity and intensity. Southern China is a humid region where
667 evapotranspiration is mainly controlled by energy supply because soil moisture is
668 usually ~~sufficient~~ not limiting. ~~For given adequate~~ In cases of low soil moisture at the
669 ~~the initiation~~ beginning of a drought, evaporative demand can increase rapidly during a
670 short period ~~when~~ if strong, transient meteorological changes (such as extreme
671 temperature) occur, which in turn ~~exhaust~~ deplete soil moisture ~~to~~ and thus intensify
672 drought conditions (Zhang et al., 2019, Otkin et al., 2018). Moreover, vegetation over

673 southern China is usually abundant and plants tend to suck more water from the soil
674 ~~when high~~ during high temperatures, ~~occur~~, causing evapotranspiration increase and
675 soil moisture decline (Li et al., 2020c; Wang et al., 2016). As a consequence, the More
676 ~~surface~~ sensible heat ~~fluxes~~ flux increases, leading to ~~are thus transferred to the near-~~
677 ~~surface atmosphere to further increase~~ increasing air temperatures (Mo and Lettenmaier,
678 2015). These land-atmosphere interactions ~~altogether~~ cause the Bowen ratio to increase
679 (Otkin et al., 2013, 2018), creating ~~a~~ favorable conditions for short-term concurrence
680 of droughts and ~~hot~~ heatwaves. Therefore, compound dry-hot events with high severity
681 and intensity ~~is~~ are more likely to occur in humid regions ~~with higher severity and~~
682 ~~intensity~~.

683 Figure 12 illustrates how well compound event characteristics are captured by
684 climate models. On average, climate models overestimate compound dry-hot frequency
685 in particular for western China, suggesting frequencies that are up to 6 times higher
686 than observations (Fig. 12a). In the east, biases are much small but still show an
687 overestimation. Climate models also generally over-estimate the duration of and
688 severity of compound dry-hot events, in particular in the west of China, whereas both
689 characteristics are better captured in the east (Fig. 12b, c). Relatively small biases are
690 present for the intensity of compound dry-hot event (Fig. 12d). All in all, the climate
691 models potentially strongly overestimate the occurrence of compound dry-hot events
692 in China, especially for western region, which is likely related to the climate models
693 overestimating the strength of the dependence between SAPEI and STI (Figure S9).
694 ~~Fig. 11 illustrates the spatial patterns of change in frequency, duration, severity, and~~
695 ~~intensity of the compound dry-hot events under the RCP 2.6, 4.5, and 8.5 scenarios for~~
696 ~~the years 2050-2100. According to Fig. 11a, the future (2050-2100) eThe compound~~
697 ~~dry-hot event frequency under all three scenarios is projected to increase in most of east~~

698 China will increase by about one to three times with respect to the reference period
699 (1961–2018). Under the RCP 8.5 scenario, compound dry-hot event at covering about
700 4% of the study region is are expected to markedly increase by more than five times,
701 which are scattered mostly in the central to west parts of China. The duration of
702 compound dry-hot event across the east of the study region will mainly show an
703 increase of about 0.5 times, while duration in mid-west China potentially increases by
704 approximately 1.5 times under RCP 8.5 scenarios (Fig. 11b). The spatial pattern of
705 future severity change is similar to the duration; severity in most of east China is
706 projected to increase by about 0.5 time under three scenarios; however, compound dry-
707 hot event severity over mid-west China is expected to more than triple under RCP 8.5
708 (Fig. 11c). The compound dry-hot event intensity in most of the study region exhibits
709 slight increase for all scenarios in comparison to the historical period. s in most areas
710 under all three scenarios

711 Global warming is very likely to exacerbate the prevalence of the compound dry-hot
712 events (Pfleiderer et al., 2019). The cCumulative density functions of the future
713 variations in compound dry-hot event characteristics considering only temperature and
714 compared to all variables changes were quantified, and the result isare shown in Fig.
715 12. The frequency and intensity of the future variations in compound dry-hot event do
716 not show large difference between two scenarioscases, while duration and severity
717 display great large increase due to when only temperature variationchanges are
718 considered, as marked evident by the movement towards the right side of the
719 cumulative density curves.

720 Given the identified biases in climate models in the dependence between SAPEI
721 and STI, multivariate bias adjustment methods are required to reliably estimate future
722 climate risk of compound events in China (Francois et al., 2020). —Increasing

723 ~~temperature could lead to remarkable increase evapotranspiration, and thus causing~~
724 ~~more surface sensible heat fluxes into atmosphere (Mo and Lettenmaier, 2015; Zhang~~
725 ~~et al., 2019). These land atmosphere interactions altogether cause the Bowen ratio to~~
726 ~~increase (Otkin et al., 2013, 2018), creating can create a favorable condition for~~
727 ~~concurrence dries and hots (Otkin et al., 2013, 2018). In short, temperature could be~~
728 ~~generally the primary factor increasing the compound dry hot severity and duration~~
729 ~~(Cook et al., 2014). In addition, trends are often present in individual variables, while~~
730 ~~can also occur in the dependence between drivers of compound events, which~~
731 ~~consequently affects associated risks. The~~Furthermore, this dependence may also
732 change under warmer conditions. For instance, the (negative) correlation between
733 seasonal mean summer temperature and precipitation is projected to intensify in many
734 land regions, which could lead to more frequent dry and hot extremes in addition to
735 long-term trends in temperature and precipitation ~~ing to more frequent extremely dry~~
736 ~~and hot conditions (Kirono et al., 2017; Zscheischler and Seneviratne, 2017a2017b);~~
737 ~~while variation in compound dry hot event due to the complex interaction between~~
738 ~~climate variables requires further study (Zscheischler et al., 2020). Effective measures~~
739 ~~need to be implemented to decrease CO₂ emissions to mitigate compound events. is need~~
740 ~~further studied (Zscheischler et al., 2020). Overall, the frequency, severity, duration,~~
741 ~~and intensity of the compound dry hot events in China under global warming will~~
742 ~~increase significantly. Effective measures need to be implemented to decrease the CO₂~~
743 ~~emissions for compound event. dry and hot event mitigation.~~

744 **4 Conclusions**

745 ~~Under global warming, Short-term the compound dry and hot events tends to be~~
746 ~~more frequent and short lived (i.e., days or weeks)~~can cause substantial damage.

747 Correspondingly, a compound drought and heat index should be able to monitor such

748 event at sub-monthly scales in order to timely reflect the evolution of concurrent dry
749 and hot conditions evolution. In this study, we developed a multiple time scale (e.g., 3-,
750 6-, 9, and 12- month) compound drought and heat index, termed as SCDHI, to monitor
751 both short-~~time-term~~ (e.g., days or weeks) and long-~~time-term~~ (e.g., months) compound
752 events. This index was established based on ~~the a~~ daily drought index (~~i.e.~~, SAPEI) and
753 the Standardized Temperature Index (STI) using a joint probability distribution method.
754 Using the SCDHI, we ~~then quantitatively investigated the~~ quantified key characteristics
755 (i.e., frequency, intensity, severity, and duration) of ~~the~~ compound dry-hot events in
756 China in the historical period (1961-2018), and ~~revealed~~ investigated how well climate
757 models simulate these characteristics. how they would change in the future (2050-2100)
758 ~~under representative concentration pathway (RCP) 2.6, 4.5, and 8.5 scenarios~~. The main
759 conclusions of this study are presented as follows: The SCDHI can ~~well~~-monitor
760 simultaneous ~~dries-dry~~ and ~~hots~~ conditions ~~detected by SAPEI and STI~~ during historic
761 high-impact events. ~~Hereby, the~~ The monthly SCDHI can provide an overall situation
762 of the compound dry and hot conditions, ~~but whereas the~~ sub-monthly SCDHI can well
763 capture fluctuation of simultaneous ~~dries-droughts~~ and ~~hots-heatwaves~~ within a month.
764 SCDHI is further a good indicator of compound dry and hot conditions on vegetation
765 health. It also can also reflect the impact of the compound dry and hot events on
766 ~~vegetation anomalies~~ health. ~~The SCDHI can offer a new tool to quantitatively measure~~
767 ~~the characteristics of the compound dry hot events. It also can provide detailed~~
768 ~~information such as the initiation, development, decay, and tendency of the compound~~
769 ~~event for decision makers and stakeholders to make early and timely warning~~. In the
770 case ~~study of the~~ China, ~~the southern China~~ the south suffered ~~more frequent the~~
771 compound dry-hot events most frequently, with generally higher severity and intensity.
772 On average, The e compound dry-hot events mainly exceeding the light category

773 typically lasted for ~~twenty-20~~five to ~~thirty-five~~35 days ~~in China~~. Climate models tend
774 to e-overestimate the frequency, duration and severity of compound dry-hot events
775 particularly in the western region of China. In conclusion, the SCDHI offers a new tool
776 to quantitatively measure the characteristics of compound dry-hot events and can
777 provide detailed information on the initiation, development and decay of such events
778 for decision-makers and stakeholders. ~~-will intensify throughout the China in the future.~~
779 ~~The frequency generally ranged from 0 to 2 times in most of study areas, while the~~
780 ~~duration and severity biases were about 0 to 1 times. will increase by about one to three~~
781 ~~times with respect to the reference period. A region with fewer compound event (<5)~~
782 ~~would exhibit a multi-fold (more than five times) increase in the future. The duration~~
783 ~~across east areas mainly increased by 0.5 times, while severity project to increase by~~
784 ~~about 0.5 to 1 times.~~

785
786
787
788 **Data availability.** The observed meteorological datasets are available at
789 <http://cdc.nmic.cn/home.do>. The CMIP5 datasets are available at <https://esgf.llnl.gov>.

790
791 **Author Contributions.** Conceived and designed the experiments: JL, SW. Performed
792 the experiments: JL, SW. Analyzed the data: JL. Wrote and edited the paper: JL, SW,
793 ZW, JZ, SG, XC.

794
795 **Competing interests.** The authors declare that they have no conflict of interest.

796

797 **Acknowledgement**

798 The research is financially supported by the National Natural Science Foundation
799 of China (51879107, 51709117), the Guangdong Basic and Applied Basic Research
800 Foundation (2019A1515111144), and the Water Resource Science and Technology
801 Innovation Program of Guangdong Province (2020-29). [JZ acknowledges the Swiss
802 National Science Foundation \(grant no. 179876\) and the Helmholtz Initiative and
803 Networking Fund \(Young Investigator Group COMPOUNDX, grant agreement VH-
804 NG-1537\).](#)

805

806

807

808

809

810

811

812

813

814

815

816

817

818 **References**

819 Allen, R. G., Pereira, L. S., Raes, D. and Smith, M.: Crop evapotranspiration:
820 Guidelines for computing crop requirements, Irrig. Drain. Pap. No. 56, FAO,
821 doi:10.1016/j.eja.2010.12.001, 1998.

822 Ayantobo, O. O., Li, Y., Song, S., Javed, T. and Yao, N.: Probabilistic modelling of
823 drought events in China via 2-dimensional joint copula, J. Hydrol., 559, 373–391,
824 doi:10.1016/j.jhydrol.2018.02.022, 2018.

825 Barton, D. E., Abramovitz, M. and Stegun, I. A.: Handbook of Mathematical Functions
826 with Formulas, Graphs and Mathematical Tables., J. R. Stat. Soc. Ser. A,
827 doi:10.2307/2343473, 1965.

828 Bi, H., Ma, J., Zheng, W. and Zeng, J.: Comparison of soil moisture in GLDAS model
829 simulations and in situ observations over the Tibetan Plateau, J. Geophys. Res.,
830 doi:10.1002/2015JD024131, 2016.

831 Chen, L., Chen, X., Cheng, L., Zhou, P. and Liu, Z.: Compound hot droughts over
832 China: Identification, risk patterns and variations, Atmos. Res., 227(May), 210–
833 219, doi:10.1016/j.atmosres.2019.05.009, 2019.

834 Cook, B. I., Smerdon, J. E., Seager, R., and Coats, S.: Global warming and 21 st century
835 drying. Climate Dynamics, 43(9-10), 2607-2627, 2014.

836 Feng, X., Fu, B., Piao, S., Wang, S., Ciais, P., Zeng, Z., Lü, Y., Zeng, Y., Li, Y., Jiang,
837 X. and Wu, B.: Revegetation in China’s Loess Plateau is approaching sustainable
838 water resource limits, Nat. Clim. Chang., doi:10.1038/nclimate3092, 2016.

839 Ford, T. W., McRoberts, D. B., Quiring, S. M. and Hall, R. E.: On the utility of in situ
840 soil moisture observations for flash drought early warning in Oklahoma, USA,
841 Geophys. Res. Lett., doi:10.1002/2015GL066600, 2015.

842 [François, B., Vrac, M., Cannon, A. J., Robin, Y. and Allard, D.: Multivariate bias](#)
843 [corrections of climate simulations: which benefits for which losses?. Earth System](#)
844 [Dynamics, 2020, 11\(2\), 537-562.](#)

845 Hao, Z., Hao, F., Singh, V. P., Xia, Y., Shi, C. and Zhang, X.: A multivariate approach
846 for statistical assessments of compound extremes, J. Hydrol., 565, 87–94,
847 doi:10.1016/j.jhydrol.2018.08.025, 2018a.

848 Hao, Z., Hao, F., Singh, V. P. and Zhang, X.: Quantifying the relationship between
849 compound dry and hot events and El Niño–southern Oscillation (ENSO) at the

850 global scale, *J. Hydrol.*, 567, 332–338, doi:10.1016/j.jhydrol.2018.10.022, 2018b.

851 Hao, Z., Hao, F., Singh, V. P. and Zhang, X.: Statistical prediction of the severity of
852 compound dry-hot events based on El Niño-Southern Oscillation, *J. Hydrol.*, 572,
853 243–250, doi:10.1016/j.jhydrol.2019.03.001, 2019.

854 [Haqiqi, I., Grogan, D. S., Hertel, T. W. and Schlenker, W.: Quantifying the Impacts of](#)
855 [Compound Extremes on Agriculture and Irrigation Water Demand. *Hydrology and*](#)
856 [Earth System Sciences Discussions, 2020, 1-52.](#)

857 [Herr, H. D., and Krzysztofowicz, R.: Generic probability distribution of rainfall in](#)
858 [space: The bivariate model. *Journal of Hydrology*, 306\(1-4\), 234-263, 2005.](#)

859 [Hansen, J., Sato, M., Ruedy, R.: Perception of climate change. *Proceedings of the*](#)
860 [National Academy of Sciences, 109\(37\), E2415-E2423, 2012.](#)

861 Hunt, E. D., Hubbard, K. G., Wilhite, D. A., Arkebauer, T. J. and Dutcher, A. L.: The
862 development and evaluation of a soil moisture index. *Int. J. Climatol.*, 29(5), 747-
863 759, doi.org/10.1002/joc.1749, 2009.

864 James, S., Complex, B., Black, S. J., Health, O. and Ando, H.: The synergy between
865 drought and extremely hot summers in the Mediterranean, *Biochem. J.*, 2010.

866 Jiang, D., Tian, Z. and Lang, X.: Reliability of climate models for China through the
867 IPCC Third to Fifth Assessment Reports, *Int. J. Climatol.*, doi:10.1002/joc.4406,
868 2016.

869 Kirono, D. G. C., Hennessy, K. J. and Grose, M. R.: Increasing risk of months with low
870 rainfall and high temperature in southeast Australia for the past 150 years, *Clim.*
871 *Risk Manag.*, doi:10.1016/j.crm.2017.04.001, 2017.

872 Koster, R. D., Schubert, S. D., Wang, H., Mahanama, S. P. and Deangelis, A. M.: Flash
873 drought as captured by reanalysis data: Disentangling the contributions of
874 precipitation deficit and excess evapotranspiration, *J. Hydrometeorol.*,

- 875 doi:10.1175/JHM-D-18-0242.1, 2019.
- 876 ~~Liang, X., Wood, E. F., and Lettenmaier, D. P.: Surface soil moisture parameterization~~
877 ~~of the VIC-2L model: Evaluation and modification. Global and Planetary Change,~~
878 ~~13(1-4), 195-206, 1996.~~
- 879 Li, C., Singh, V. P., & Mishra, A. K. (2013). A bivariate mixed distribution with a
880 heavy-tailed component and its application to single-site daily rainfall simulation.
881 Water Resources Research, 49(2), 767-789.
- 882 Li, B., H. Beaudoin, and M. Rodell, 2018: GLDAS Catchment Land Surface Model
883 L4 daily 0.25 3 0.25 degree V2.0 (GLDAS_CLSM025_D) at GES DISC. GES
884 DISC, 6 August 2019, <https://doi.org/10.5067/LYHA9088MFWQ>
- 885 Li, J., Wang, Z., Wu, X., Chen, J., Guo, S., and Zhang, Z.: A new framework for
886 tracking flash drought events in space and time. *Catena*, 194, 104763, 2020a.
- 887 Li, J., Wang, Z., Wu, X., Xu, C.-Y., Guo, S. and Chen, X.: Toward Monitoring Short-
888 Term Droughts Using a Novel Daily-Scale, Standardized Antecedent Precipitation
889 Evapotranspiration Index, *J. Hydrometeorol.*, 891–908, doi:10.1175/jhm-d-19-
890 0298.1, 2020b.
- 891 Li, J., Wang, Z., Wu, X., Guo, S., and Chen, X.: Flash droughts in the Pearl River Basin,
892 China: Observed characteristics and future changes. *Sci. Total Environ.*, 707,
893 136074, 2020c.
- 894 Lin, W., Wen, C., Wen, Z. and Gang, H.: Drought in Southwest China: A Review,
895 *Atmos. Ocean. Sci. Lett.*, 8(6), 339–344, doi:10.3878/AOSL20150043, 2015.
- 896 Liu, Z., Wang, Y., Shao, M., Jia, X., Li, X: Spatiotemporal analysis of multiscalar
897 drought characteristics across the Loess Plateau of China. *J. Hydrol.*, 534, 281-
898 299, doi.org/10.1016/j.jhydrol.2016.01.003, 2016,
- 899 Liu, Y., Zhu, Y., Ren, L., Singh, V. P., Yang, X. and Yuan, F.: A multiscalar Palmer

900 drought severity index, *Geophys. Res. Lett.*, 44(13), 6850–6858,
901 doi:10.1002/2017GL073871, 2017.

902 Liu, Y., Zhu, Y., Ren, L., Yong, B., Singh, V. P., Yuan, F., Jiang, S. and Yang, X.: On
903 the mechanisms of two composite methods for construction of multivariate
904 drought indices, *Sci. Total Environ.*, 647, 981–991,
905 doi:10.1016/j.scitotenv.2018.07.273, 2019.

906 Liu, Y., Zhu, Y., Zhang, L., Ren, L., Yuan, F., Yang, X. and Jiang, S.: Flash droughts
907 characterization over China: From a perspective of the rapid intensification rate,
908 *Sci. Total Environ.*, doi:10.1016/j.scitotenv.2019.135373, 2020.

909 Lu, E.: Determining the start, duration, and strength of flood and drought with daily
910 precipitation: Rationale, *Geophys. Res. Lett.*, 36(12), 1–5,
911 doi:10.1029/2009GL038817, 2009.

912 Lu, E., Cai, W., Jiang, Z., Zhang, Q., Zhang, C., Higgins, R. W. and Halpert, M. S.:
913 The day-to-day monitoring of the 2011 severe drought in China, *Clim. Dyn.*, 43(1–
914 2), 1–9, doi:10.1007/s00382-013-1987-2, 2014.

915 [Luan, X. and Vico, G.: Canopy temperature and heat stress are increased by compound](#)
916 [high air temperature and water stress, and reduced by irrigation—A modeling](#)
917 [analysis. *Hydrology and Earth System Sciences Discussions*, 2021, 1-22.](#)

918 [McKee, T. B., Doesken, N. J., and Kleist, J.: The relationship of drought frequency and](#)
919 [duration to time scales. In *Proceedings of the 8th Conference on Applied*](#)
920 [Climatology \(Vol. 17, No. 22, pp. 179-183\), 1993.](#)

921 Mo, K. C. and Lettenmaier, D. P.: Heat wave flash droughts in decline, *Geophys. Res.*
922 *Lett.*, doi:10.1002/2015GL064018, 2015.

923 Mo, K. C. and Lettenmaier, D. P.: Precipitation deficit flash droughts over the United
924 States, *J. Hydrometeorol.*, doi:10.1175/JHM-D-15-0158.1, 2016.

925 Mazdiyasi, O. and AghaKouchak, A.: Substantial increase in concurrent droughts and
926 heatwaves in the United States, *Proc. Natl. Acad. Sci. U. S. A.*, 112(37), 11484–
927 11489, doi:10.1073/pnas.1422945112, 2015.

928 Manning, C., Widmann, M., Bevacqua, E., Van Loon, A. F., Maraun, D. and Vrac, M:
929 Increased probability of compound long-duration dry and hot events in Europe
930 during summer (1950-2013). *Environmental Research Letters*, 14(9), 094006,
931 2019.

932 Osman, M., Zaitchik, B. F., Badr, H. S., Christian, J. I., Tadesse, T., Otkin, J. A. and
933 Anderson, M. C.: Flash drought onset over the Contiguous United States:
934 Sensitivity of inventories and trends to quantitative definitions, *Hydrol. Earth Syst.*
935 *Sci. Discuss.*, doi.org/10.5194/hess-2020-385, in review, 2020.

936 Otkin, J. A., Anderson, M. C., Hain, C., Mladenova, I. E., Basara, J. B. and Svoboda,
937 M.: Examining rapid onset drought development using the thermal infrared-based
938 evaporative stress index, *J. Hydrometeorol.*, doi:10.1175/JHM-D-12-0144.1, 2013.

939 Otkin, J. A., Svoboda, M., Hunt, E. D., Ford, T. W., Anderson, M. C., Hain, C. and
940 Basara, J. B.: Flash droughts: A review and assessment of the challenges imposed
941 by rapid-onset droughts in the United States, *Bull. Am. Meteorol. Soc.*, 99(5),
942 911–919, doi:10.1175/BAMS-D-17-0149.1, 2018.

943 [Pendergrass, A. G., Meehl, G. A., Pulwarty, R., Hobbins, M., Hoell, A., AghaKouchak,](#)
944 [A. and Woodhouse, C. A.: Flash droughts present a new challenge for](#)
945 [subseasonal-to-seasonal prediction. *Nature Climate Change*, 2020, 10\(3\), 191-199.](#)

946 Pflleiderer, P., Schleussner, C. F., Kornhuber, K. and Coumou, D.: Summer weather
947 becomes more persistent in a 2 °C world, *Nat. Clim. Chang.*, 9(9), 666–671,
948 doi:10.1038/s41558-019-0555-0, 2019.

949 [Ridder, N. N., Pitman, A. J., Westra, S., Ukkola, A., Do Hong, X., Bador, M., and](#)

950 [Zscheischler, J.: Global hotspots for the occurrence of compound events. Nature](#)
951 [communications, 11\(1\), 1-10, 2020.](#)

952 Rodell, M., Houser, P. R., Jambor, U., Gottschalck, J., Mitchell, K., Meng, C. J.,
953 Arsenault, K., Cosgrove, B., Radakovich, J., Bosilovich, M., Entin, J. K., Walker,
954 J. P., Lohmann, D. and Toll, D.: The Global Land Data Assimilation System, Bull.
955 Am. Meteorol. Soc., doi:10.1175/BAMS-85-3-381, 2004.

956 [Ridder, N. N., Pitman, A. J., Westra, S., Ukkola, A., Do Hong, X., Bador, M. and](#)
957 [Zscheischler, J.: Global hotspots for the occurrence of compound events. Nature](#)
958 [communications, 11\(1\), 1-10, 2020.](#)

959 ~~Röthlisberger, M. and Martius, O.: Quantifying the Local Effect of Northern~~
960 ~~Hemisphere Atmospheric Blocks on the Persistence of Summer Hot and Dry~~
961 ~~Spells, Geophys. Res. Lett., doi:10.1029/2019GL083745, 2019.~~

962 Schumacher, D. L., Keune, J., van Heerwaarden, C. C., Vilà-Guerau de Arellano, J.,
963 Teuling, A. J. and Miralles, D. G.: Amplification of mega-heatwaves through heat
964 torrents fuelled by upwind drought, Nat. Geosci., 12(9), 712–717,
965 doi:10.1038/s41561-019-0431-6, 2019.

966 Sedlmeier, K., Feldmann, H. and Schädler, G.: Compound summer temperature and
967 precipitation extremes over central Europe, Theor. Appl. Climatol.,
968 doi:10.1007/s00704-017-2061-5, 2018.

969 Stagge, J. H., Tallaksen, L. M., Gudmundsson, L., Van Loon, A. F. and Stahl, K.:
970 Candidate Distributions for Climatological Drought Indices (SPI and SPEI), Int. J.
971 Climatol., doi:10.1002/joc.4267, 2015.

972 ~~Seneviratne, S. I., Corti, T., Davin, E. L., Hirschi, M., Jaeger, E. B., Lehner, I., and~~
973 ~~Teuling, A. J.: Investigating soil moisture-climate interactions in a changing~~
974 ~~climate: A review. Earth Science Reviews, 99(3-4), 125-161, 2010.~~

975 ~~Sun, C. and Yang, S.: Persistent severe drought in southern China during winter-spring~~
976 ~~2011: Large-scale circulation patterns and possible impacting factors, J. Geophys.~~
977 ~~Res. Atmos., doi:10.1029/2012JD017500, 2012.~~

978 Sun, C. X., Huang, G. H., Fan, Y., Zhou, X., Lu, C. and Wang, X. Q.: Drought
979 Occurring With Hot Extremes: Changes Under Future Climate Change on Loess
980 Plateau, China, *Earth's Futur.*, 7(6), 587–604, doi:10.1029/2018EF001103, 2019.

981 Swain, D. L., Langenbrunner, B., Neelin, J. D. and Hall, A.: Increasing precipitation
982 volatility in twenty-first-century California, *Nat. Clim. Chang.*, 8(5), 427–433,
983 doi:10.1038/s41558-018-0140-y, 2018.

984 Taylor, K. E., Stouffer, R. J. and Meehl, G. A.: An overview of CMIP5 and the
985 experiment design, *Bull. Am. Meteorol. Soc.*, doi:10.1175/BAMS-D-11-00094.1,
986 2012.

987 Terzi, S., Torresan, S., Schneiderbauer, S., Critto, A., Zebisch, M. and Marcomini, A.:
988 Multi-risk assessment in mountain regions: A review of modelling approaches for
989 climate change adaptation, *J. Environ. Manage.*, 232(September 2018), 759–771,
990 doi:10.1016/j.jenvman.2018.11.100, 2019.

991 Vicente-Serrano, S. M., Beguería, S. and López-Moreno, J. I.: A multiscalar drought
992 index sensitive to global warming: The standardized precipitation
993 evapotranspiration index, *J. Clim.*, 23(7), 1696–1718,
994 doi:10.1175/2009JCLI2909.1, 2010.

995 [Villalobos-Herrera, R., Bevacqua, E., Ribeiro, A. F., Auld, G., Crocetti, L., Mircheva,](#)
996 [B. and De Michele, C.: Towards a compound event-oriented climate model](#)
997 [evaluation: A decomposition of the underlying biases in multivariate fire and heat](#)
998 [stress hazards. *Natural Hazards and Earth System Sciences Discussions*, 2020, 1-](#)
999 [31.](#)

- 1000 Wang, L., Yuan, X., Xie, Z., Wu, P. and Li, Y.: Increasing flash droughts over China
1001 during the recent global warming hiatus, *Sci. Rep.*, doi:10.1038/srep30571, 2016.
- 1002 Wang, W., Wang, W. J., Li, J. S., Wu, H., Xu, C. and Liu, T.: The impact of sustained
1003 drought on vegetation ecosystem in southwest China based on remote sensing, in
1004 *Procedia Environmental Sciences.*, 2010.
- 1005 [Wang, Z., Zhong, R., Lai, C., Zeng, Z., Lian, Y. and Bai, X.: Climate change enhances](#)
1006 [the severity and variability of drought in the Pearl River Basin in South China in](#)
1007 [the 21st century. *Agricultural and Forest Meteorology*, 2018, 249, 149-162.](#)
- 1008 Werner, A. T. and Cannon, A. J.: Hydrologic extremes - An intercomparison of multiple
1009 gridded statistical downscaling methods, *Hydrol. Earth Syst. Sci.*,
1010 doi:10.5194/hess-20-1483-2016, 2016.
- 1011 Winston, H.A., Ruthi, L.J.: Evaluation of RADAP II severe-storm-detection algorithms.
1012 *Bull. Am. Meteorol. Soc.*, 67(2), 145-150, doi.org/10.1175/1520-
1013 0477(1986)067<0145:EORISS>2.0.CO;2 1986.
- 1014 Wu, J., Chen, X., Yao, H., Liu, Z. and Zhang, D.: Hydrological Drought Instantaneous
1015 Propagation Speed Based on the Variable Motion Relationship of Speed-Time
1016 Process, *Water Resour. Res.*, doi:10.1029/2018WR023120, 2018.
- 1017 Wu, X., Hao, Z., Hao, F. and Zhang, X.: Variations of compound precipitation and
1018 temperature extremes in China during 1961–2014, *Sci. Total Environ.*, 663, 731–
1019 737, doi:10.1016/j.scitotenv.2019.01.366, 2019.
- 1020 Wu, X., Hao, Z., Zhang, X., Li, C. and Hao, F.: Evaluation of severity changes of
1021 compound dry and hot events in China based on a multivariate multi-index
1022 approach, *J. Hydrol.*, 583, 124580, doi:10.1016/j.jhydrol.2020.124580, 2020.
- 1023 ~~Xia, Y., Moeko, D. M., Wang, S., Pan, M., Kumar, S. V., and Peters-Lidard, C. D.:~~
1024 ~~Comprehensive evaluation of the variable infiltration capacity (VIC) model in the~~

1025 ~~North American Land Data Assimilation System. Journal of Hydrometeorology,~~
1026 ~~19(11), 1853–1879, 2018.~~

1027 Xu, C., McDowell, N. G., Fisher, R. A., Wei, L., Sevanto, S., Christoffersen, B. O.,
1028 Weng, E. and Middleton, R. S.: Increasing impacts of extreme droughts on
1029 vegetation productivity under climate change, Nat. Clim. Chang., 9(12), 948–953,
1030 doi:10.1038/s41558-019-0630-6, 2019.

1031 Xu, K., Yang, D., Yang, H., Li, Z., Qin, Y. and Shen, Y.: Spatio-temporal variation of
1032 drought in China during 1961–2012: A climatic perspective, J. Hydrol.,
1033 doi:10.1016/j.jhydrol.2014.09.047, 2015.

1034 Yang, Y., Bai, L., Wang, B., Wu, J. and Fu, S.: Reliability of the global climate models
1035 during 1961–1999 in arid and semiarid regions of China, Sci. Total Environ.,
1036 doi:10.1016/j.scitotenv.2019.02.188, 2019.

1037 [Yevjevich, V., and Ingenieur, J.: An Objective Approach to Definitions and](#)
1038 [Investigations of Continental Hydrologic Droughts. Water Resource Publ, Fort](#)
1039 [Collins, 1967.](#)

1040 Yeo, I. N. K. and Johnson, R. A.: A new family of power transformations to improve
1041 normality or symmetry, Biometrika, 87(4), 954–959,
1042 doi:10.1093/biomet/87.4.954, 2000.

1043 ~~Yu, H., Zhang, Q., Xu, C. Y., Du, J., Sun, P. and Hu, P.: Modified Palmer Drought~~
1044 ~~Severity Index: Model improvement and application, Environ. Int., 130(January),~~
1045 ~~104951, doi:10.1016/j.envint.2019.104951, 2019.~~

1046 Yuan, X., Wang, L., Wu, P., Ji, P., Sheffield, J. and Zhang, M.: Anthropogenic shift
1047 towards higher risk of flash drought over China, Nat. Commun.,
1048 doi:10.1038/s41467-019-12692-7, 2019.

1049 Zhang, W. J., Lu, Q. F., Gao, Z. Q. and Peng, J.: Response of remotely sensed

1050 normalized difference water deviation index to the 2006 drought of eastern
1051 Sichuan Basin, *Sci. China, Ser. D Earth Sci.*, 51(5), 748–758, doi:10.1007/s11430-
1052 008-0037-0, 2008.

1053 Zhang, Y., You, Q., Chen, C. and Li, X.: Flash droughts in a typical humid and
1054 subtropical basin: A case study in the Gan River Basin, China, *J. Hydrol.*, 551,
1055 162–176, doi:10.1016/j.jhydrol.2017.05.044, 2017.

1056 Zhang, Y., You, Q., Mao, G., Chen, C. and Ye, Z.: Short-term concurrent drought and
1057 heatwave frequency with 1.5 and 2.0 °C global warming in humid subtropical
1058 basins: a case study in the Gan River Basin, China, *Clim. Dyn.*, 52(7–8), 4621–
1059 4641, doi:10.1007/s00382-018-4398-6, 2019.

1060 Zhong, R., Chen, X., Lai, C., Wang, Z., Lian, Y., Yu, H. and Wu, X.: Drought
1061 monitoring utility of satellite-based precipitation products across mainland China,
1062 *J. Hydrol.*, 568(June 2018), 343–359, doi: 10.1016/j.jhydrol.2018.10.072, 2019a.

1063 Zhong, R., Zhao, T., He, Y. and Chen, X.: Hydropower change of the water tower of
1064 Asia in 21st century: A case of the Lancang River hydropower base, upper
1065 Mekong, *Energy*, 179, 685–696, doi:10.1016/j.energy.2019.05.059, 2019b.

1066 Zscheischler, J., Michalak, A. M., Schwalm, C., Mahecha, M. D. and Zeng, N.: Impact
1067 of large-scale climate extremes on biospheric carbon fluxes: An intercomparison
1068 based on MsTMIP data, *Global Biogeochem. Cycles*, 28(6), 585–600,
1069 doi:10.1002/2014GB004826, 2014.

1070 Zscheischler, J., Orth, R. and Seneviratne, S. I.: Bivariate return periods of temperature
1071 and precipitation explain a large fraction of European crop yields, *Biogeosciences*,
1072 doi:10.5194/bg-14-3309-2017, 2017a.

1073 Zscheischler, J. and Seneviratne, S. I.: Dependence of drivers affects risks associated
1074 with compound events, *Sci. Adv.*, 3(6), 1–11, doi:10.1126/sciadv.1700263, 2017b.

1075 Zscheischler, J., Westra, S., Van Den Hurk, B. J. J. M., Seneviratne, S. I., Ward, P. J.,
1076 Pitman, A., Aghakouchak, A., Bresch, D. N., Leonard, M., Wahl, T. and Zhang,
1077 X.: Future climate risk from compound events, *Nat. Clim. Chang.*, 8(6), 469–477,
1078 doi:10.1038/s41558-018-0156-3, 2018.

1079 Zscheischler, J., Martius, O., Westra, S., Bevacqua, E. and Raymond, C.: A typology
1080 of compound weather and climate events, *Nat. Rev. Earth Environ.*, doi:
1081 <https://doi.org/10.1038/s43017-020-0060-z>, 2020.

1082 [Zscheischler, J. and Fischer, E. M.: The record-breaking compound hot and dry 2018](#)
1083 [growing season in Germany. *Weather and climate extremes*, 2020, 29, 100270.](#)

1084 ~~Zhou, J., Wu, Z., He, H., Wang, F., Xu, Z., and Wu, X.: Regional assimilation of in situ~~
1085 ~~observed soil moisture into the VIC model considering spatial variability.~~
1086 ~~*Hydrological Sciences Journal*, 64(16), 1982–1996, 2019.~~

1087
1088
1089
1090
1091
1092
1093
1094
1095
1096
1097
1098
1099
1100
1101
1102

1103

1104

1105 **Table**

1106 Table 1 Categories of compound dry and hot conditions based on SCDHI.

Category	Dry-hot condition	SCDHI
Grade 0	Abnormal	(-0.80, -0.50]
Grade 1	Light	(-1.30, -0.80]
Grade 2	Moderate	(-1.60, -1.30]
Grade 3	Heavy	(-2.0, -1.60]
Grade 4	Extreme	≤ -2

1107

1108

1109

1110

1111

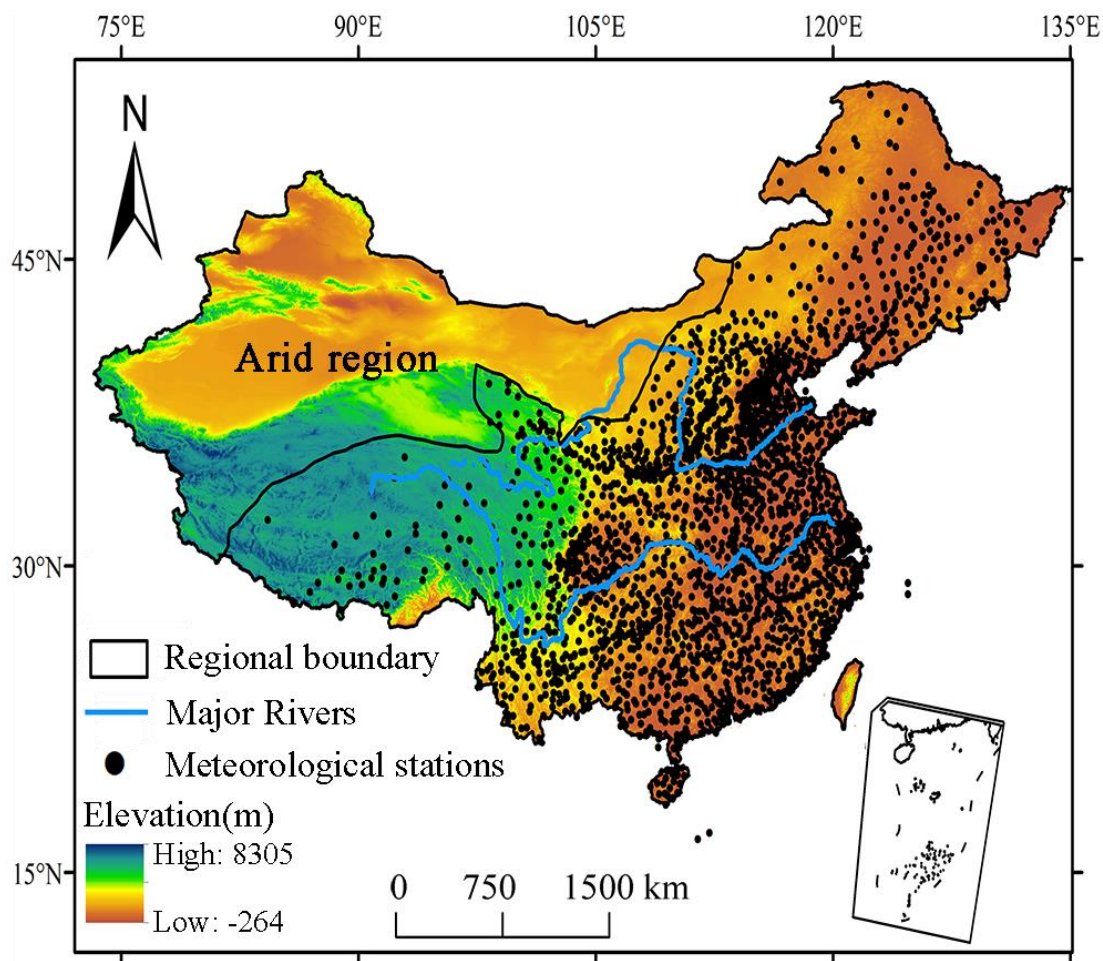
1112

1113

1114

1115

1116 **Figure**



1117

1118 Figure 1 Geographical position of China and local of meteorological stations.

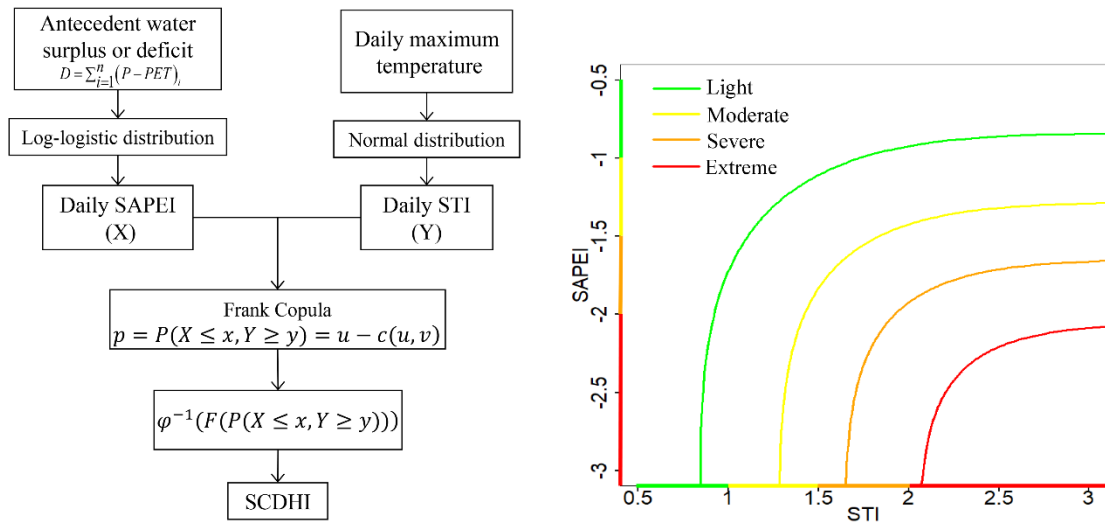
1119

1120

1121

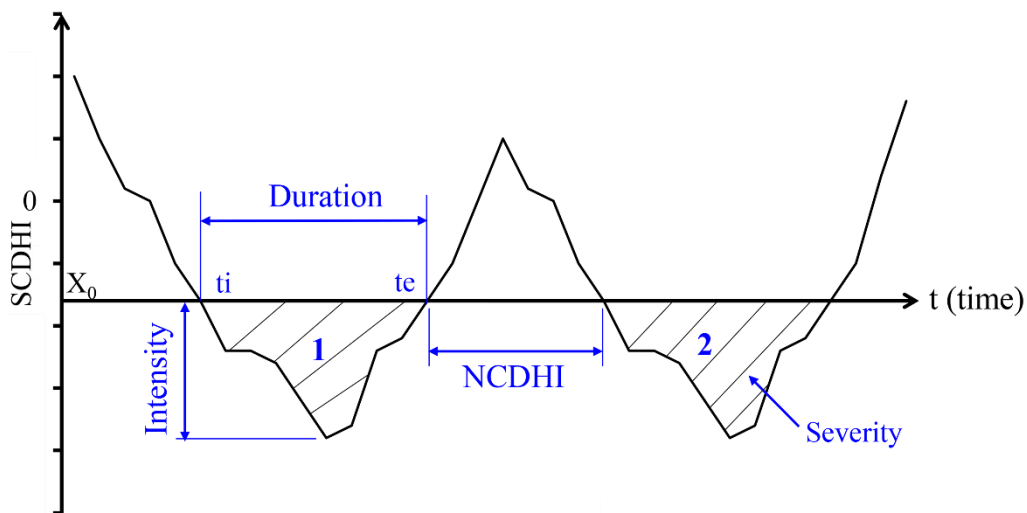
1122

1123



1124

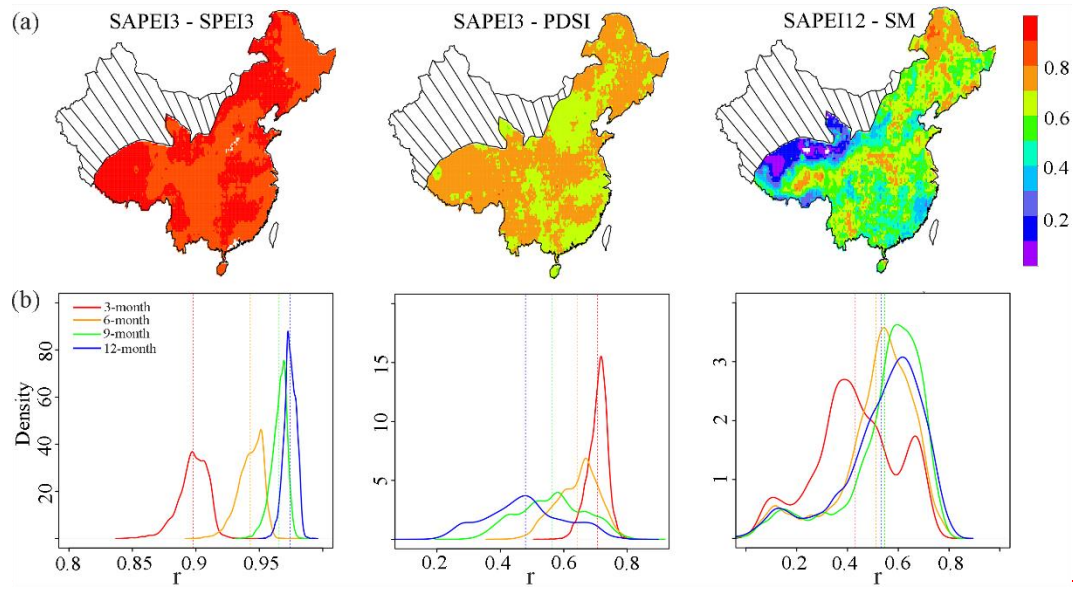
1125 Figure 2 The graphical illustration of the SCDHI construction, and the relation between
 1126 STI and SAPEI under different severity levels of compound drought and hot conditions
 1127 (given by the legend). Different colors in abscissa and ordinate represents different
 1128 drought or hot conditions (i.e., light, moderate, severe, and extreme). The isolines are
 1129 calculated from a specific calendar day, using the fitted Frank Copula with the
 1130 parameter being -1.31.



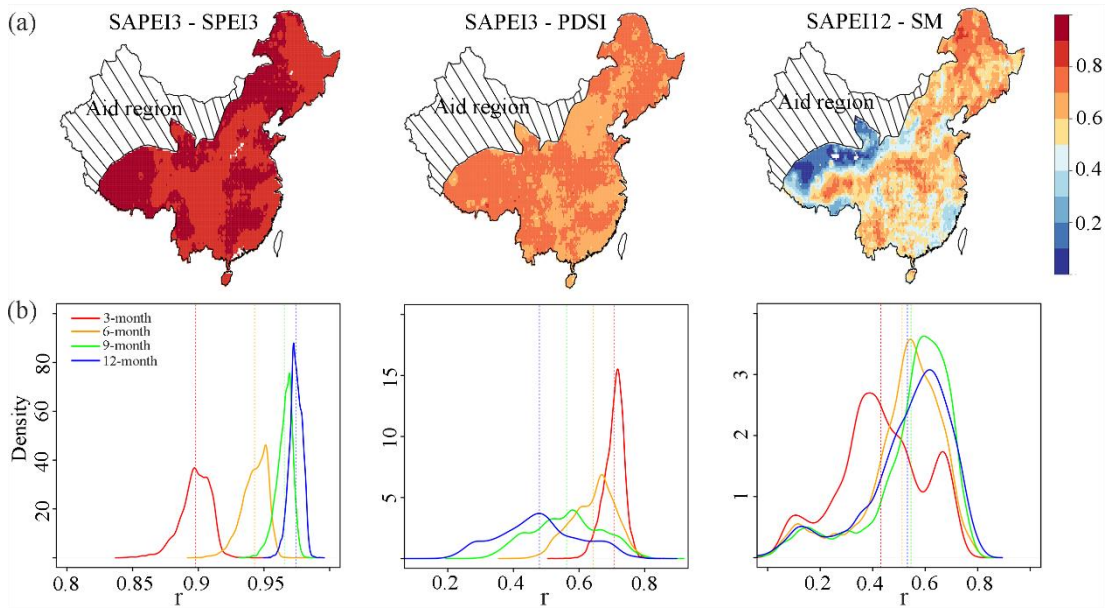
1131

1132 Figure 3 Definition sketch of characteristics of compound dry-hot event showing two
 1133 events (labeled as 1 and 2), on the basis of run theory. Note: X_0 -Truncation level,
 1134 NCDHC-Non compound dry and hot condition, t_i - initiation time, t_e -termination time.

1135



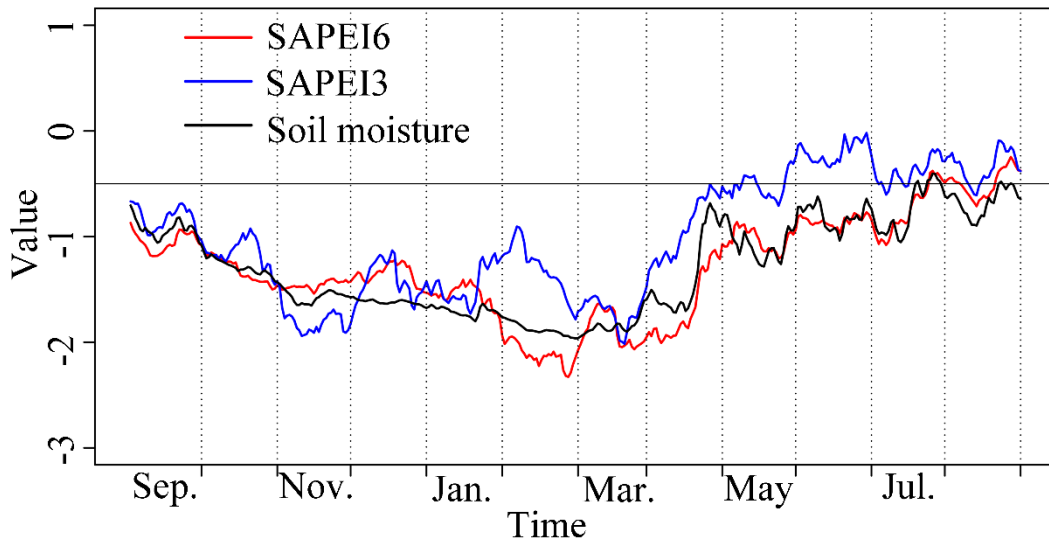
1136



1137

1138 Figure 2-4 (a) The spatial pattern of the correlations between monthly SAPEI and
 1139 SPEI/PDSI, and between daily SAPEI and soil moisture (SM), and (b) The density plot
 1140 for the correlation coefficients between SAPEI and SPEI/PDSI/SM. The monthly
 1141 SAPEI is computed by averaging the daily values in each month.

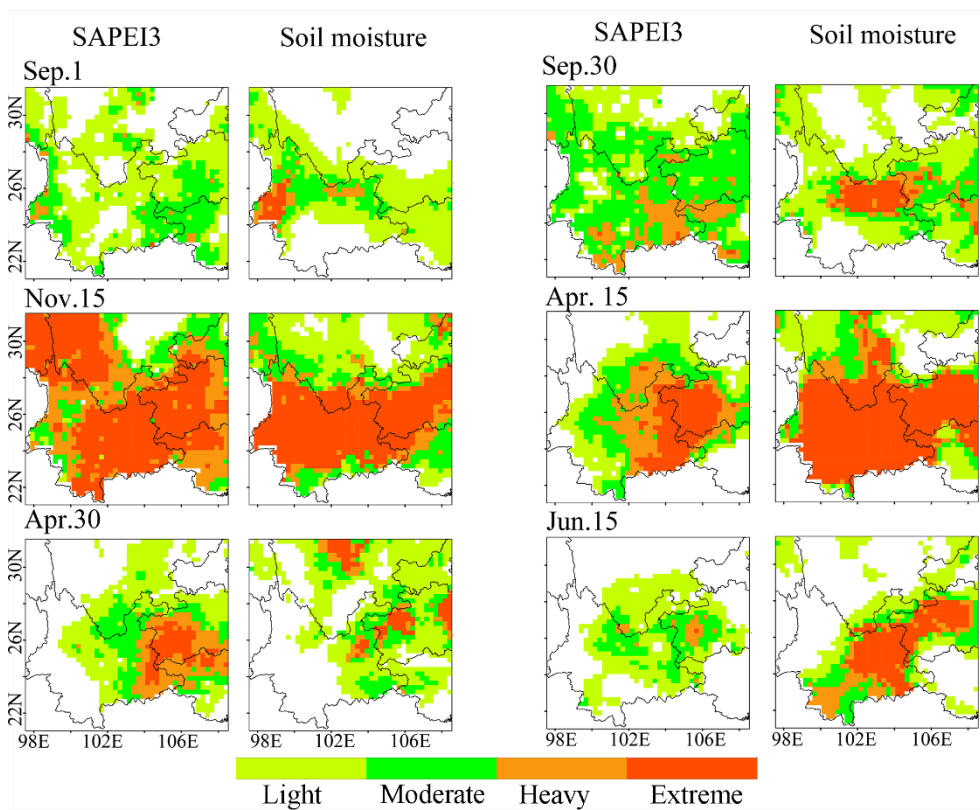
1142



1143

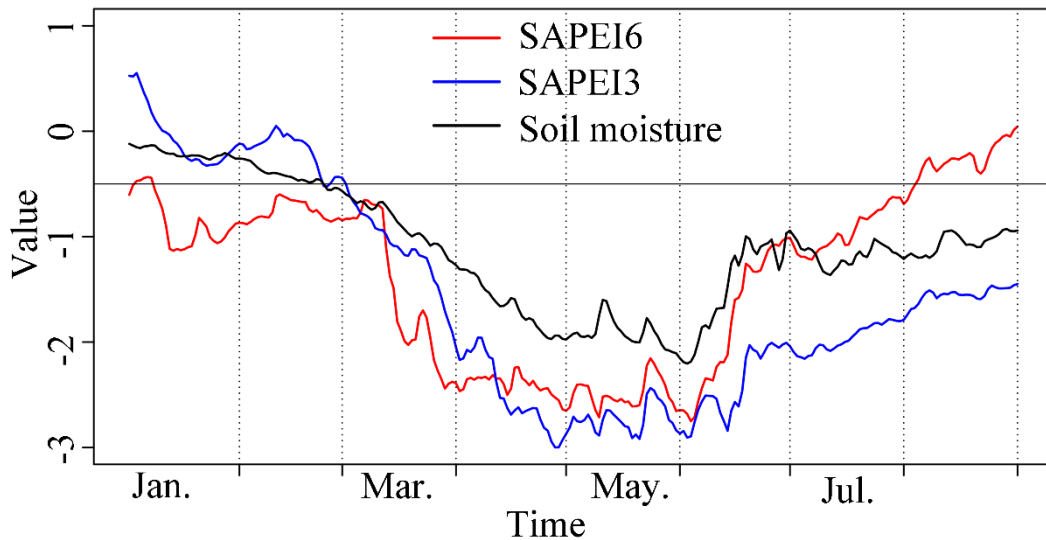
1144 Figure 3-5 SAPEI and soil moisture series during the 2009/2010 drought event over the
 1145 southwest China. ~~Shown are The series were the~~ spatially averaged merged-series. The
 1146 value of solid black line is at -0.5, indicating the distinction between drought and non-
 1147 drought conditions.

1148



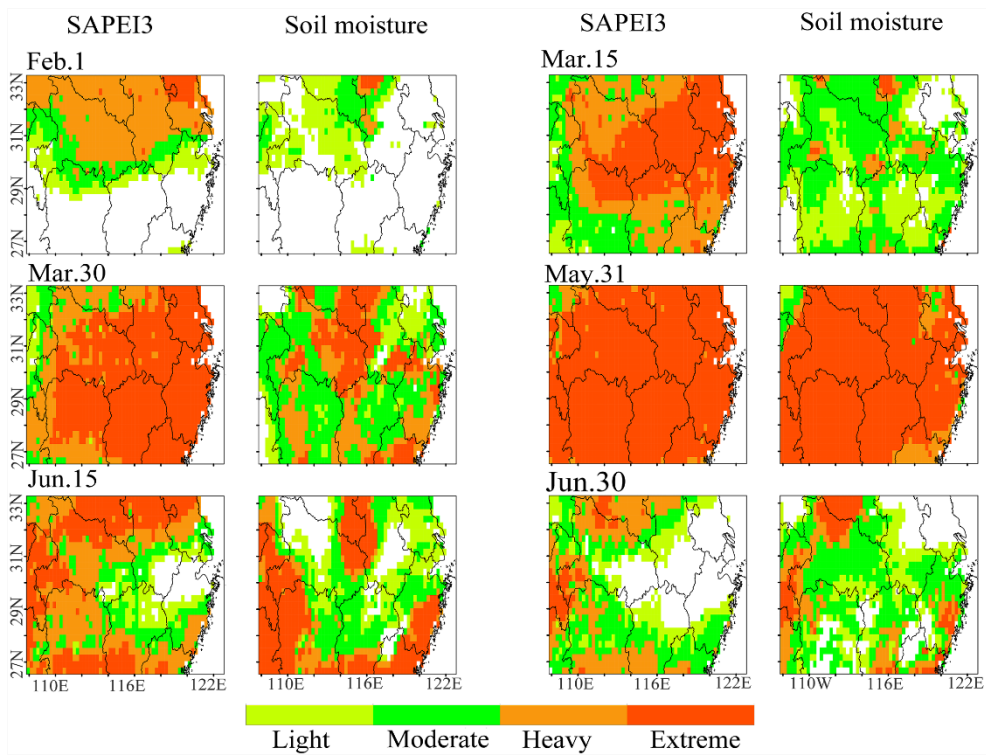
1149

1150 ~~Figure 4 Daily evolutions of the 2009/2010 drought event over the southwest China~~
 1151 ~~monitored by 3-month SAPEI and soil moisture.~~



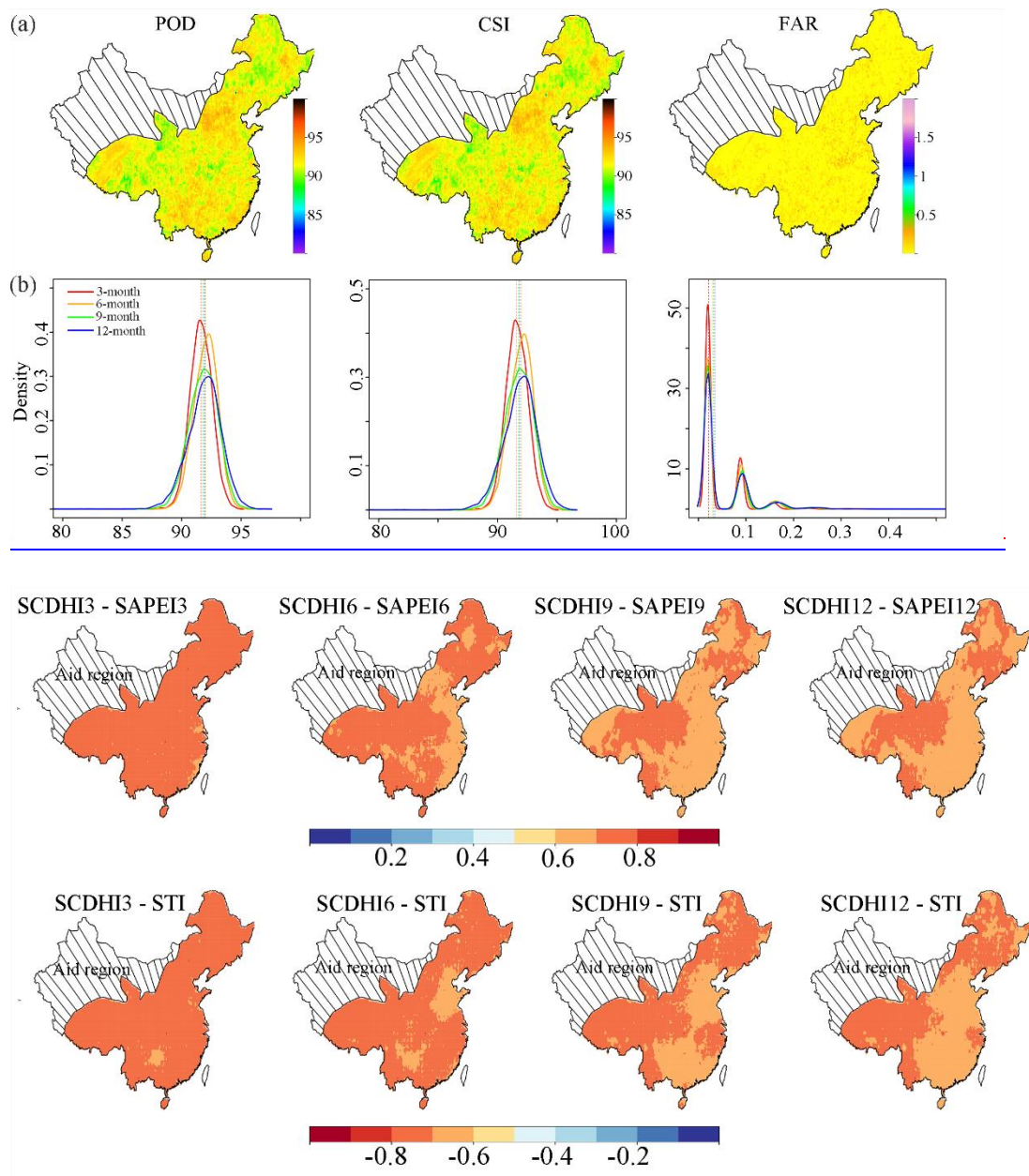
1152

1153 Figure 5-6 SAPEI (3- and 6-month) and soil moisture series during the 2011 drought
 1154 event over the middle and lower reaches of the Yangtze River. Shown are the series
 1155 were spatially averaged merged series. The value of solid black line is at -0.5, indicating
 1156 the distinction between drought and non-drought conditions.



1157

1158 Figure 6 Daily evolutions of the 2011 drought event over the middle and lower reaches
 1159 of the Yangtze River monitored by 3-month SAPEI and soil moisture.



1160

1161

1162 [Figure 7-7](#) The correlation between SAPEI/STI and SCDHI during the historical period

1163 [\(1961-2018\)](#).(a) The spatial pattern of probability of detection (POD, %), critical

1164 success index (CSI, %), and false alarm ratio (FAR, %) for 3-month SCDHI from 1961

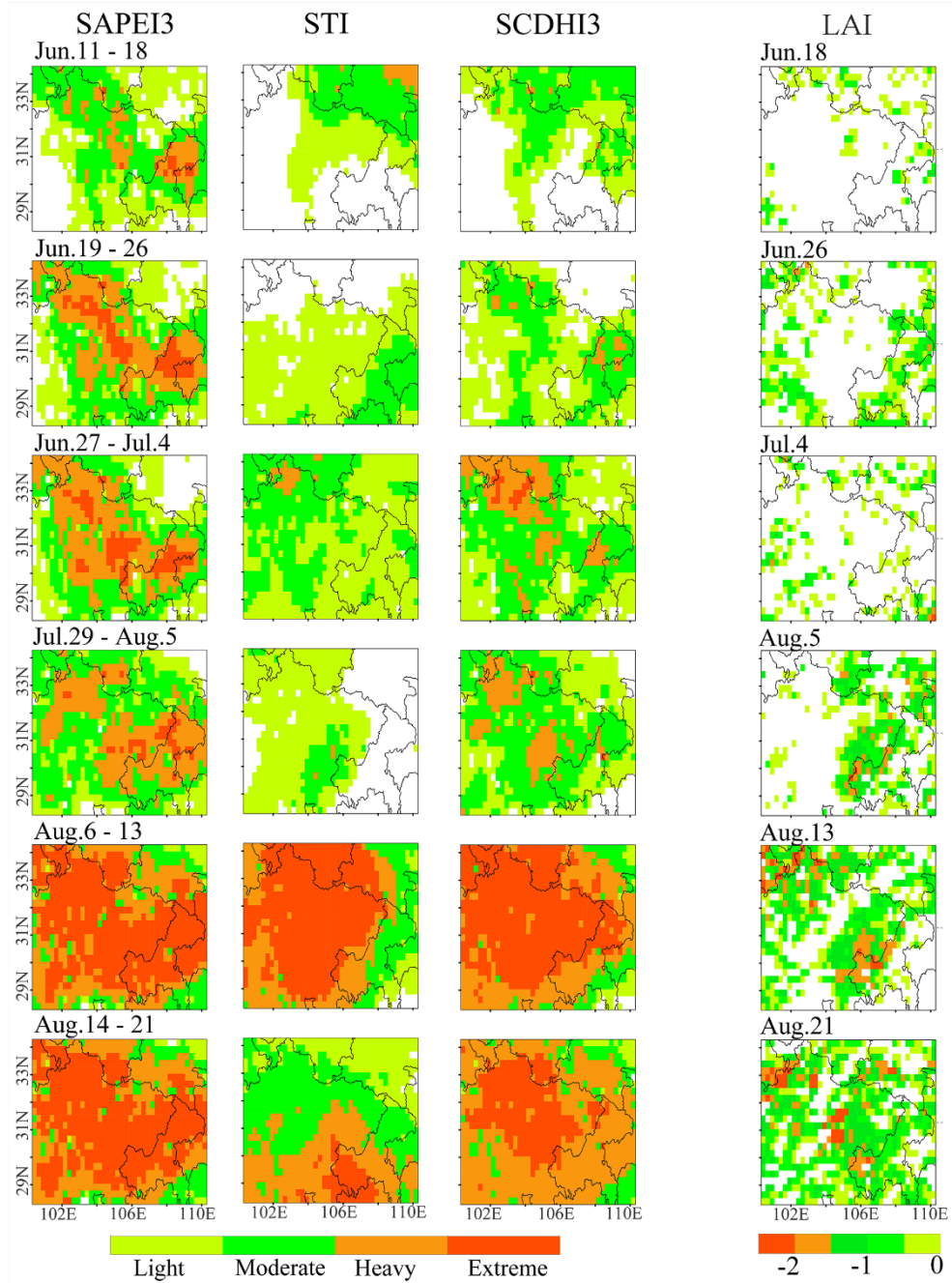
1165 to 2018, and (b) Density plot for POD, FAR, and CSI for 3-, 6-, 9-, 12-month SCDHI

1166 from 1961 to 2018.

1167

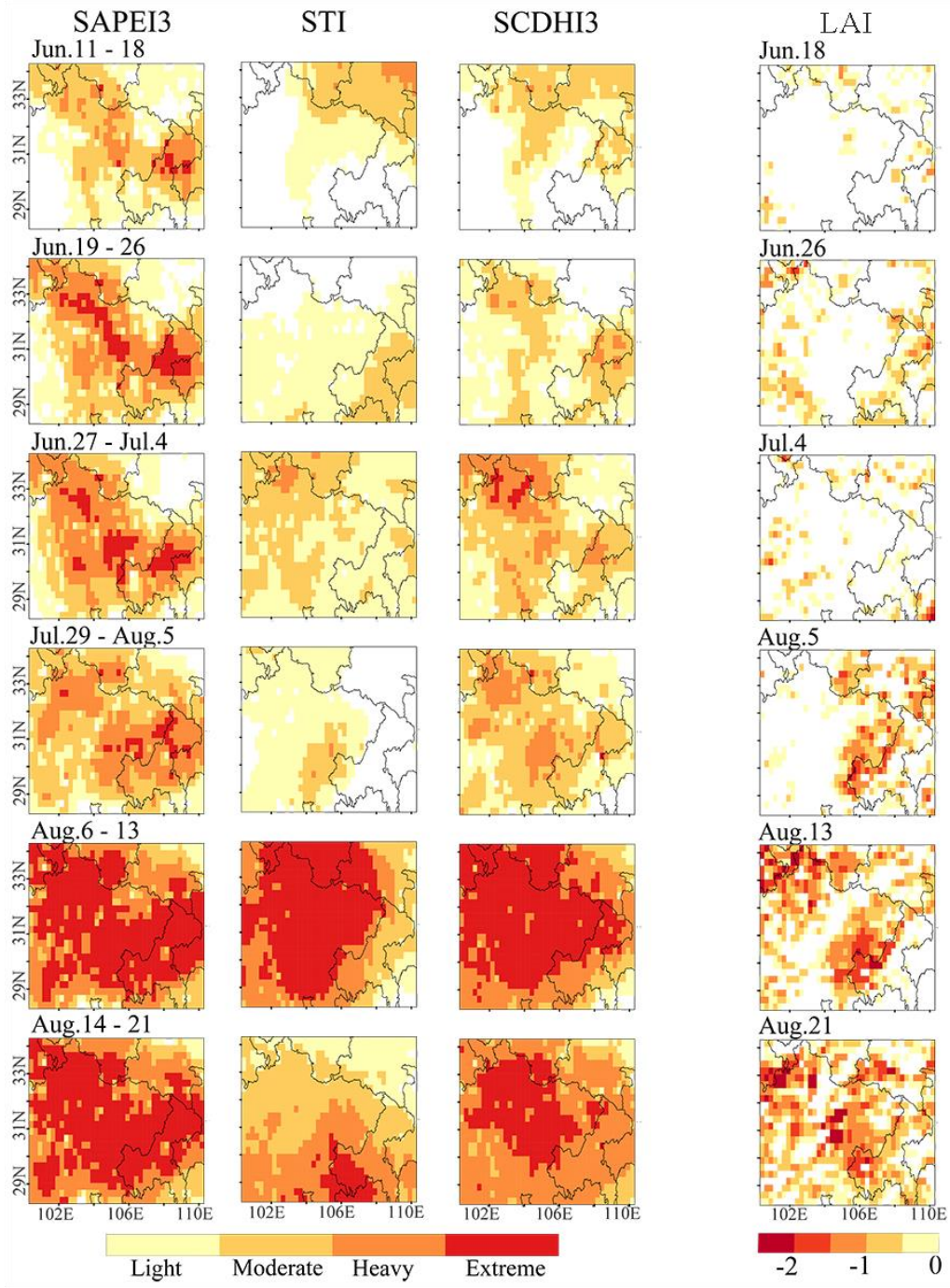
1168

1169



1170

1171



1172

1173 Figure 8 The spatial evolutions of the compound dry and hot event over the Sichuan-

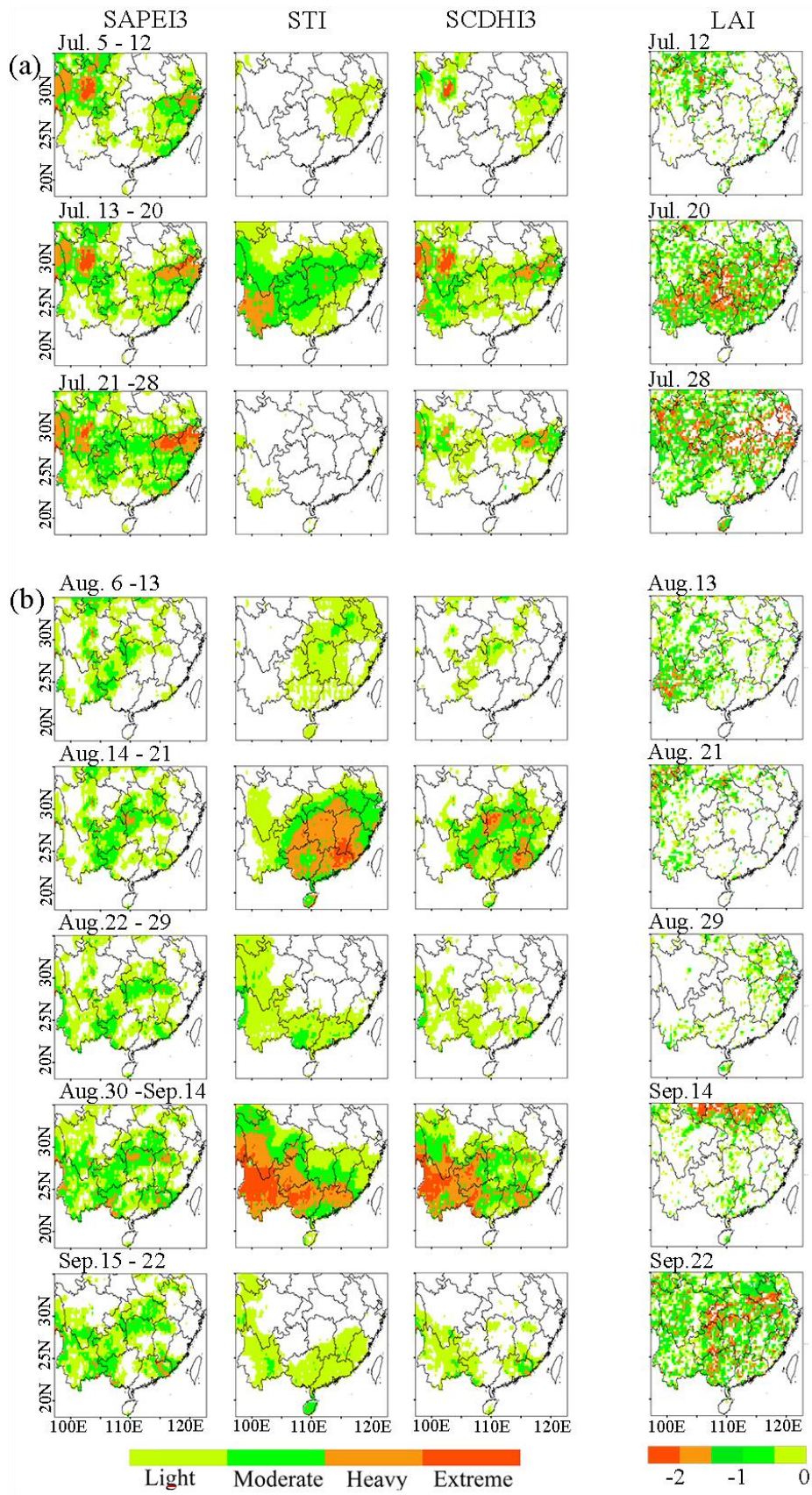
1174 Chongqing region in 2006 and its impact on vegetation [as weekly averages](#).

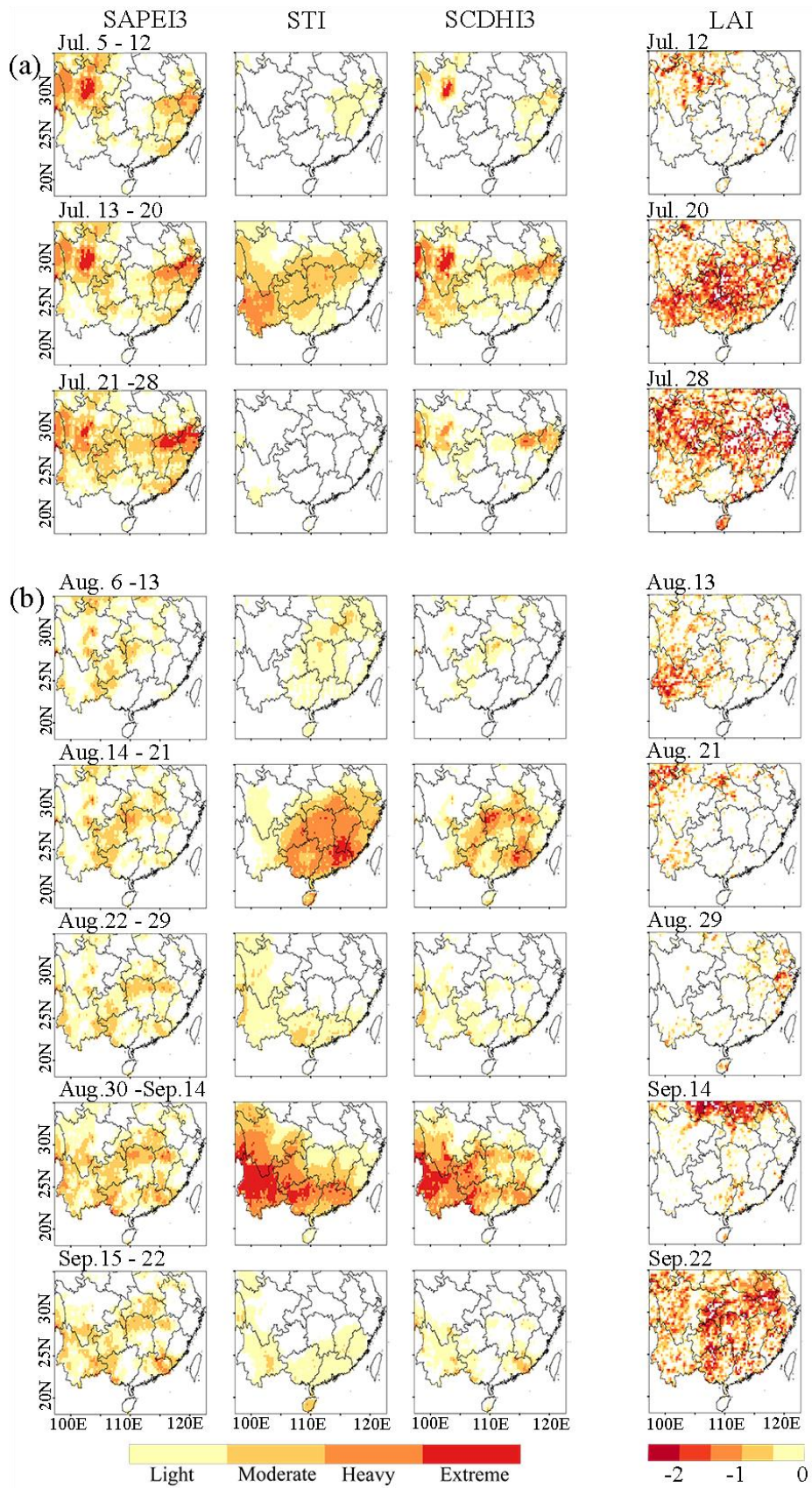
1175

1176

1177

1178

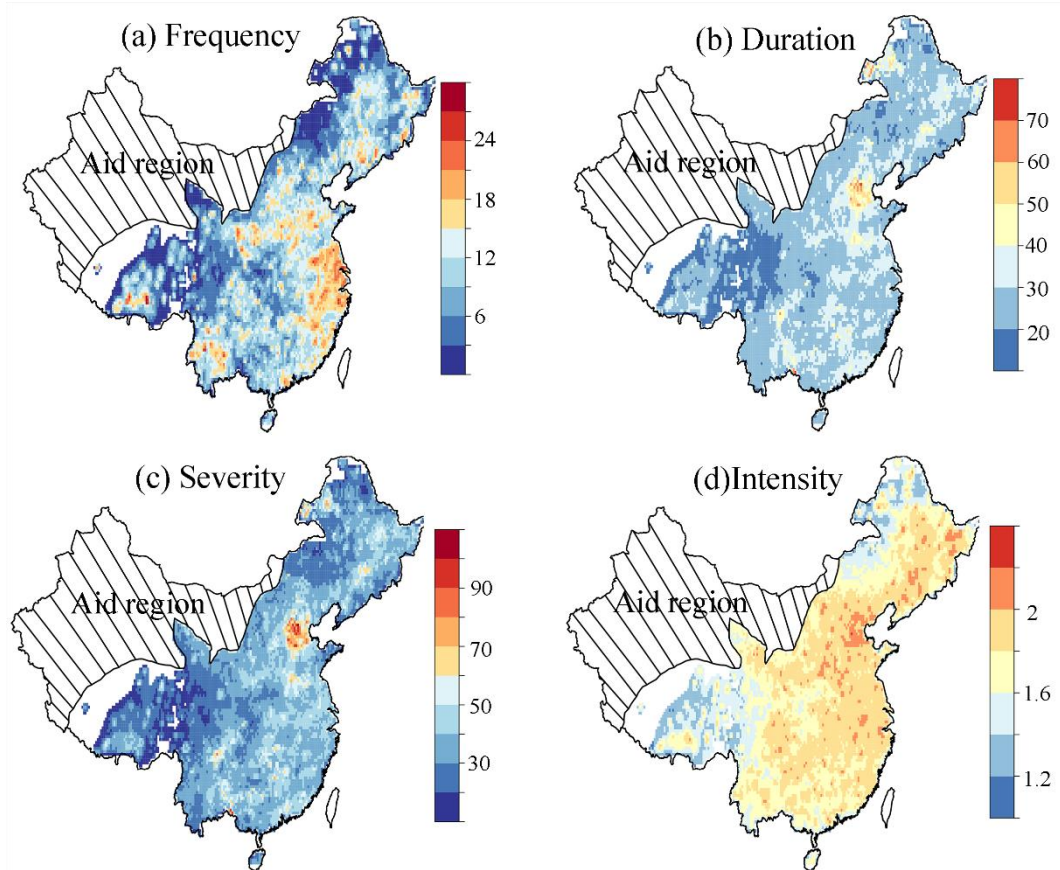
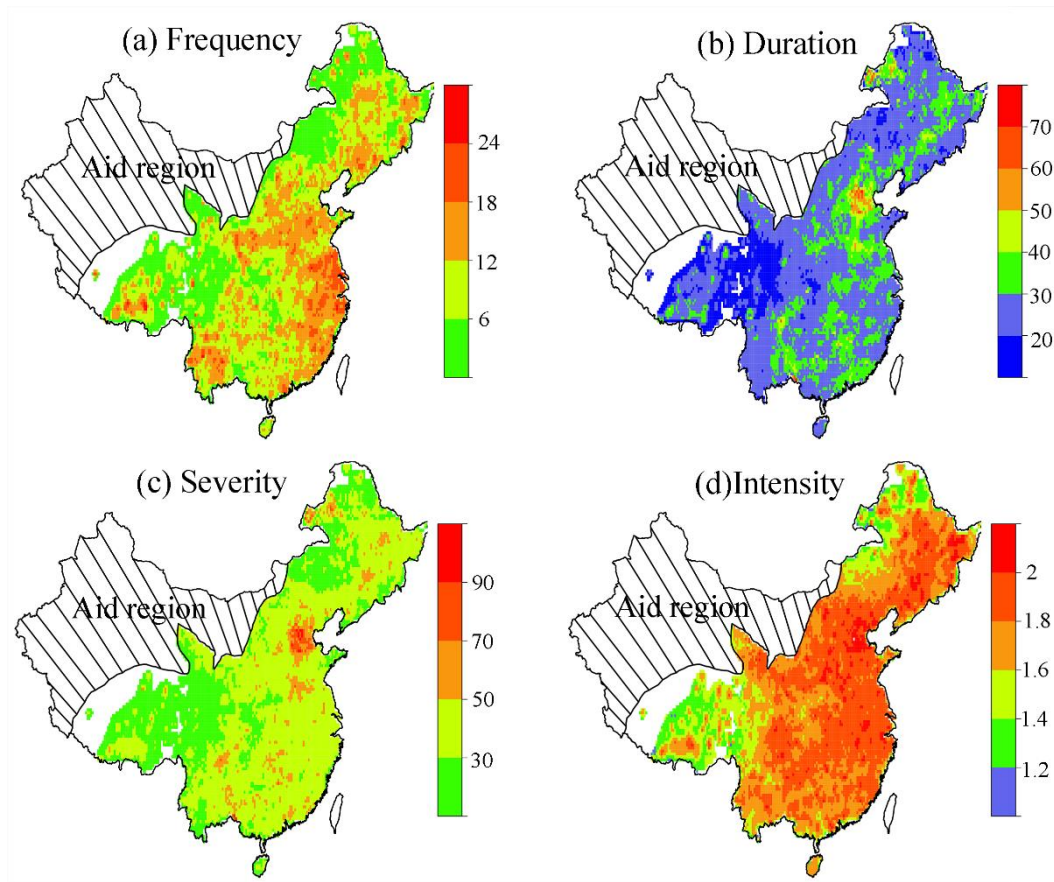




1180

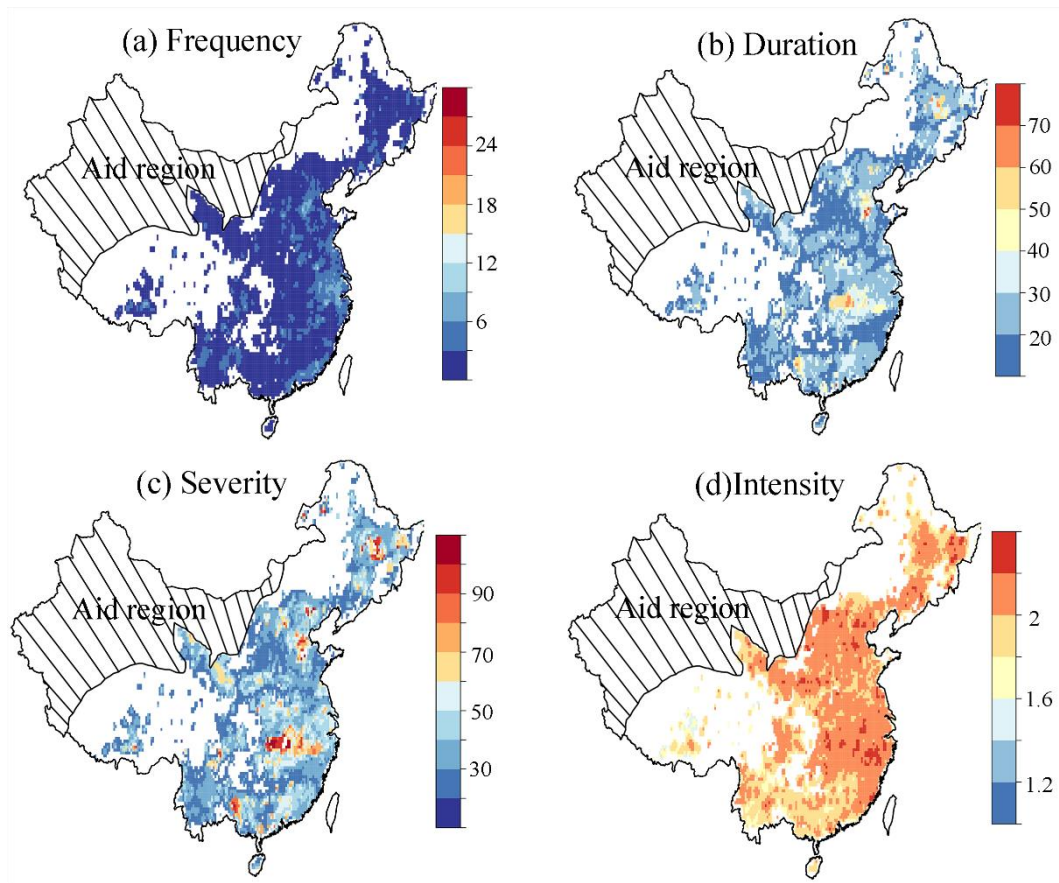
1181 Figure 9 The spatial evolutions of the compound dry and hot event over the southern

1182 China in 2009 and its impact on vegetation [as weekly averages](#).



1186 Figure 10 The spatial pattern of the key characteristics of ~~the~~ compound dry and hot
1187 events in China from 1961 to 2018, using the threshold of -0.8 in run theory. Frequency
1188 (a) refers to the total events during historical period; duration (b), severity (c), and
1189 intensity (d) are the average values of all events. White color indicates there are no
1190 events. Only events longer than two weeks are considered.

1191



1192

1193 Figure 11 The same as Figure 10, but using the threshold of -1.3 in run theory. The
1194 definition of the frequency, duration, severity, and intensity are the same as Figure 10.
1195 White color indicates there are no events.

1196

1197

1198

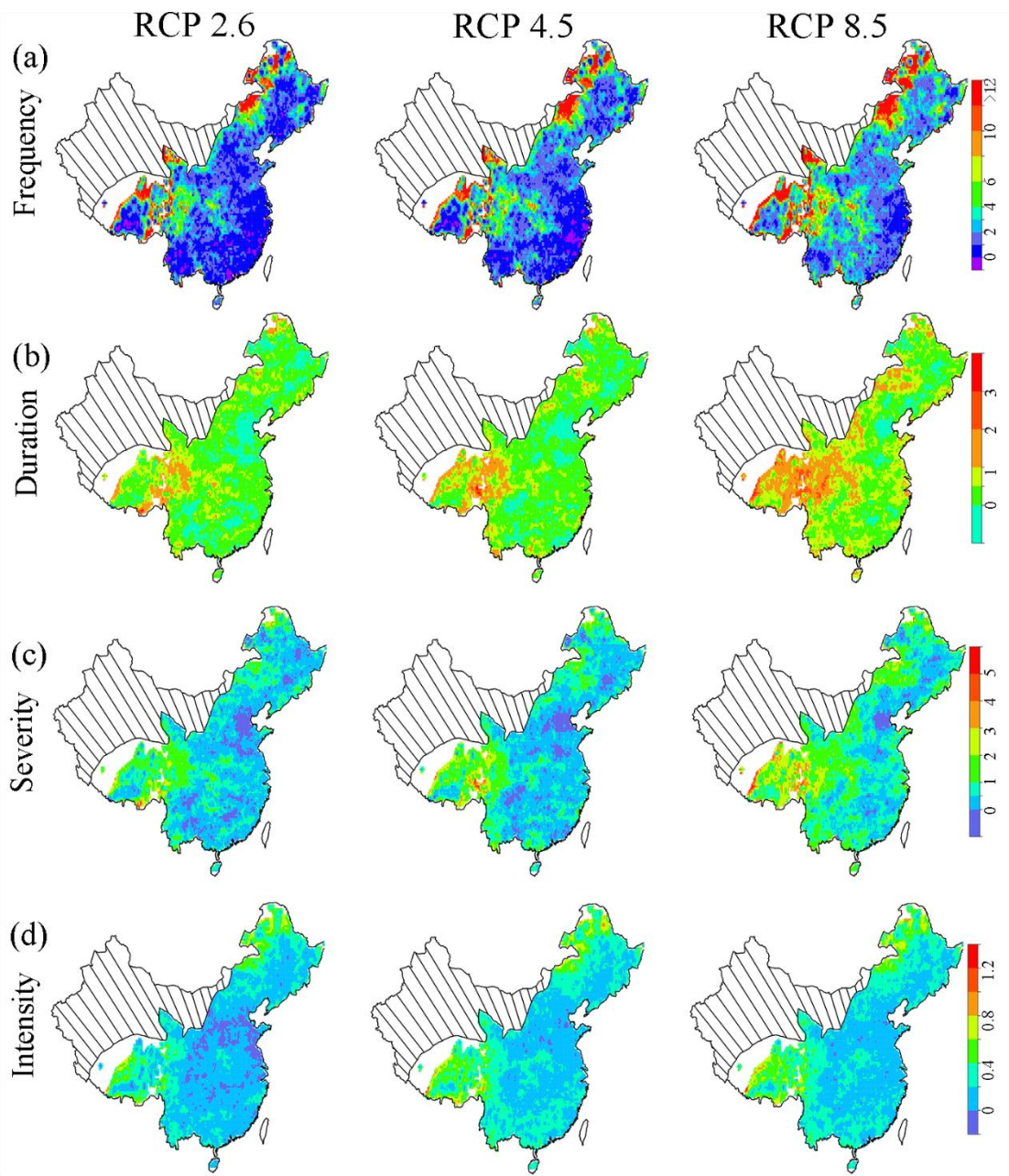
1199

1200

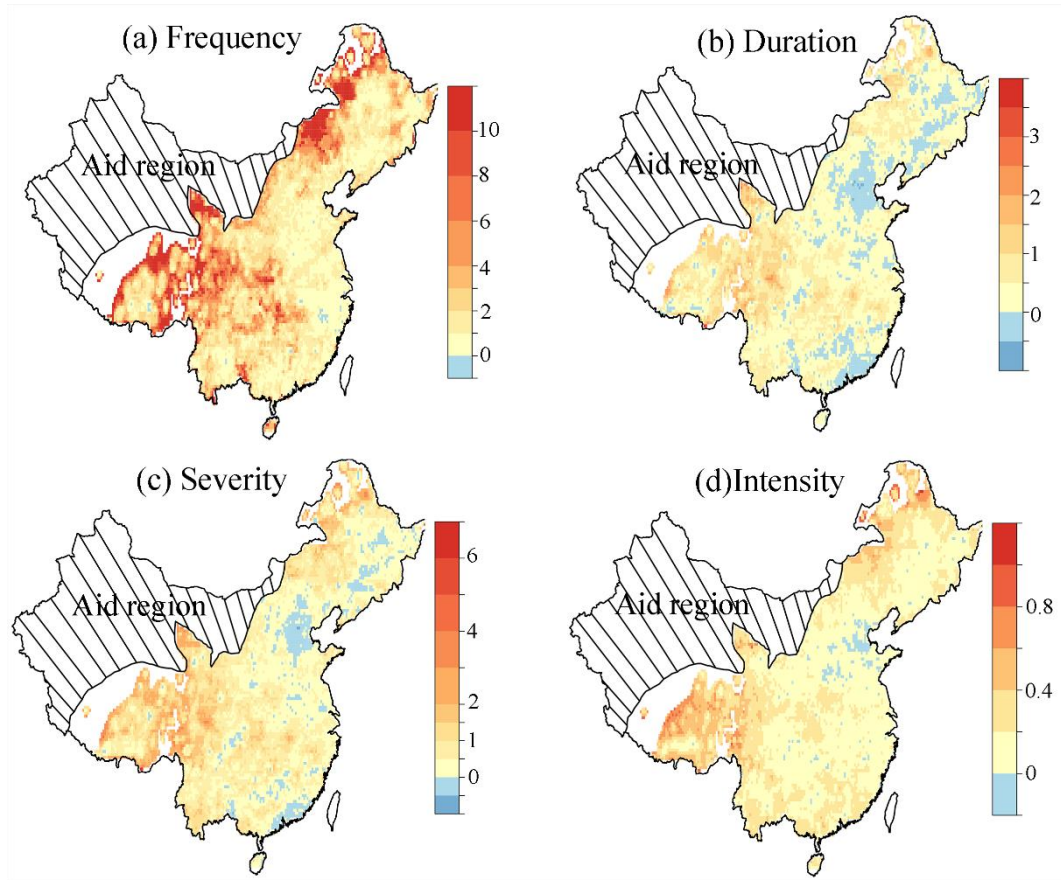
1201

1202

1203



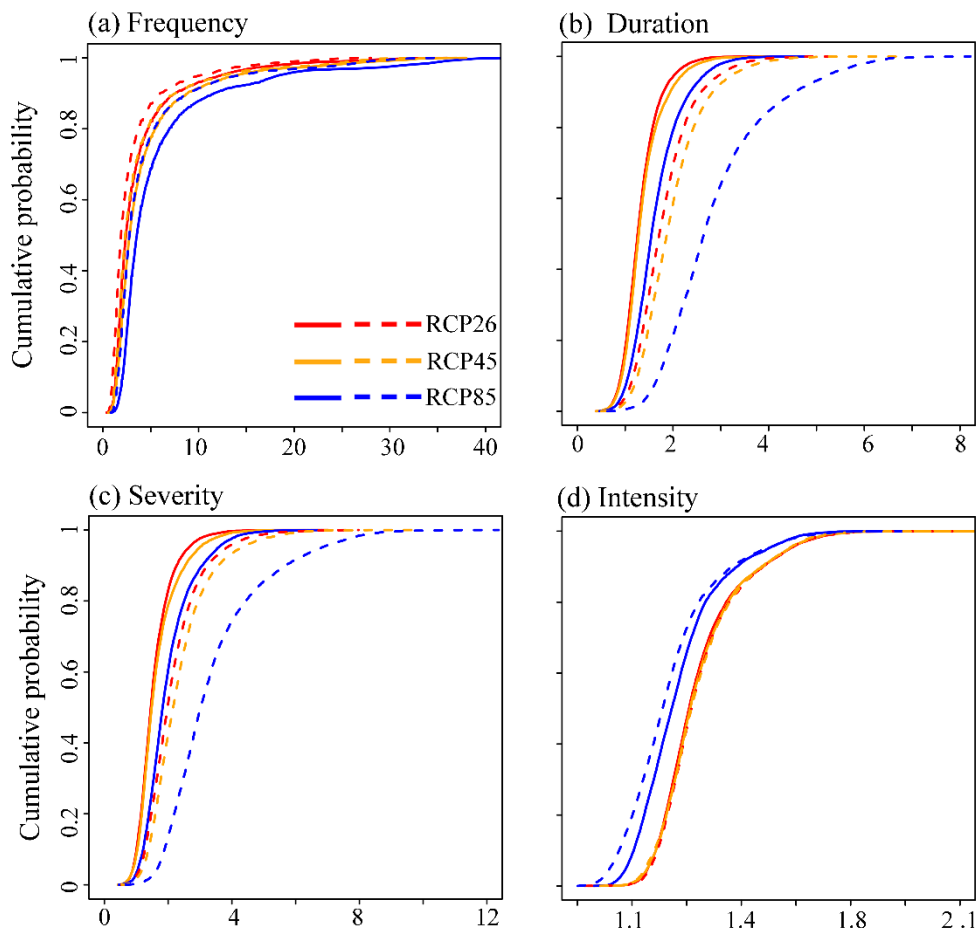
1204



1205

1206 [Figure 12 Relative climate model biases in the characteristics of the compound dry and](#)
 1207 [hot events in China. The biases are computed as the ratio of the difference between](#)
 1208 [model and observational values to the observational values. The definition of the](#)
 1209 [frequency, duration, severity, and intensity are the same as Figure 10. White color](#)
 1210 [indicates there are no events. The periods were from 1961-2005. The threshold in run](#)
 1211 [theory is -0.8. ~~Figure 11 Future changes in characteristics of the compound dry and hot~~](#)
 1212 [events under the RCP 2.6, RCP4.5 and RCP8.5 scenarios. The change values were the](#)
 1213 [ratio of the future value to the reference values. Reference period: 1961-2018, and](#)
 1214 [future period: 2050-2100.](#)

1215



1216

1217

1218

1219

1220

1221

1222

Figure 12 Cumulative probability of future changes (multiple) in of the compound dry-hot event characteristics. The dash lines indicate future characteristics changes only considered temperature change, while solid lines represent the future changes driven by all variable variation.